Oxytocin excites BNST interneurons and inhibits BNST output neurons to the central amygdala

Walter Francesconi [1,2], Fulvia Berton [1,2], Valentina Olivera-Pasilio [1,2,3], and Joanna Dabrowska [1,2,3]

[1] Center for the Neurobiology of Stress Resilience and Psychiatric Disorders, Rosalind Franklin University of Medicine and Science, North Chicago, IL 60064, USA

[2] Discipline of Cellular and Molecular Pharmacology, Chicago Medical School, Rosalind Franklin University of Medicine and Science, North Chicago, IL 60064, USA

[3] School of Graduate and Postdoctoral Studies, Rosalind Franklin University of Medicine and Science, North Chicago, IL 60064, USA

* To whom correspondence should be addressed:

Joanna Dabrowska, Center for the Neurobiology of Stress Resilience and Psychiatric Disorders, Rosalind Franklin University of Medicine and Science, North Chicago, IL 60064, USA

joanna.dabrowska@rosalindfranklin.edu

Phone: (847) 578-8664

Fax: (847) 578-3268

Number of figures (7), number of tables (1)

Highlights

- Oxytocin directly excites and increases spontaneous firing of Type I BNST interneurons
- Oxytocin indirectly inhibits Type II BNST neurons
- Oxytocin inhibits Type II BNST output neurons to the central amygdala (BNST→CeA)
- Oxytocin reduces GABA-ergic transmission in Type III BNST neurons
- Oxytocin might facilitate cued fear by inhibiting the Type II BNST→CeA neurons

Graphical abstract

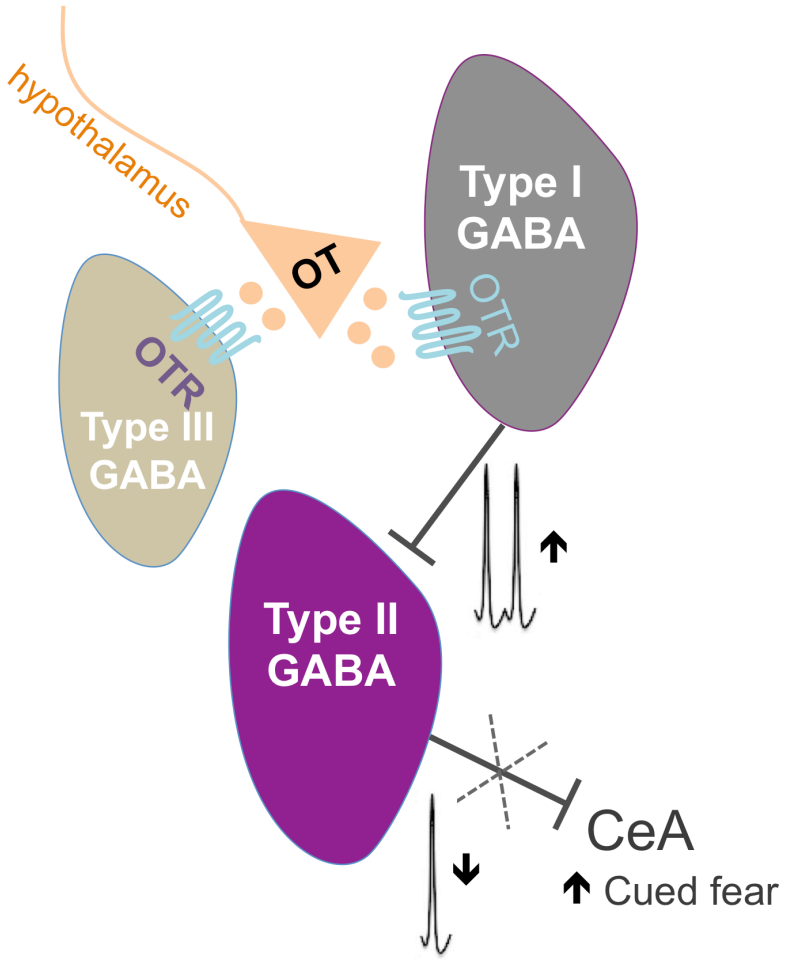

Abstract

The dorsolateral bed nucleus of the stria terminalis ($BNST_{DL}$) has high expression of oxytocin (OT) receptors (OTR), which were shown to facilitate cued fear. However, the role of OTR in the modulation of $BNST_{DL}$ activity remains elusive. $BNST_{DL}$ contains GABA-ergic neurons classified based on intrinsic membrane properties into three types. Using *in vitro* patch-clamp recordings in male rats, we demonstrate that OT selectively excites and increases spontaneous firing rate of Type I $BNST_{DL}$ neurons. As a consequence, OT increases the frequency, but not amplitude, of spontaneous inhibitory post-synaptic currents (sIPSCs) selectively in Type II neurons, an effect abolished by OTR antagonist or tetrodotoxin, and reduces spontaneous firing rate in these neurons. These results suggest an indirect effect of OT in Type II neurons, which is mediated via OT-induced increase in firing of Type I interneurons. As Type II $BNST_{DL}$ neurons were shown projecting to the central amygdala (CeA), we also recorded from retrogradelly labeled BNST→CeA neurons and we show that OT increases the frequency of sIPSC in these Type II BNST→CeA output neurons. In contrast, in Type III neurons, OT reduces the amplitude, but not frequency, of both sIPSCs and evoked IPSCs via a postsynaptic mechanism without changing their intrinsic excitability. We present a model of fine-tuned modulation of $BNST_{DL}$ activity by OT, which selectively excites $BNST_{DL}$ interneurons and inhibits Type II BNST→CeA output neurons. These results suggest that OTR in the BNST might facilitate cued fear by inhibiting the BNST→CeA neurons.

Keywords: oxytocin; BNST; central amygdala; electrophysiology, patch-clamp; cell-attached

1. Introduction

Oxytocin (OT) is a nine amino acid peptide serving as a hypothalamic hormone, which regulates uterine contractions during labor, milk ejection reflex during lactation (Caldeyro-Barcia and Poseiro, 1959; Nickerson et al., 1954), as well as water-electrolyte balance (Han et al., 1993; Verbalis et al., 1993). As a neuromodulator in the central nervous system, OT facilitates social behaviors (Bosch and Young, 2018; Pedersen et al., 1992; Tabbaa et al., 2016), regulates stress response, stress-coping behaviors, and fear and anxiety-like behaviors, for review see (Janeček and Dabrowska, 2019; Neumann and Slattery, 2016; Olivera-Pasilio and Dabrowska, 2020). Although OT has been shown to reduce fear responses primarily in the central amygdala (CeA) (Knobloch et al., 2012; Terburg et al., 2018; Viviani et al., 2011), we recently showed that oxytocin receptor (OTR) transmission in the dorsolateral bed nucleus of the stria terminalis ($BNST_{DL}$) facilitates the formation of cued fear and improves fear discrimination to signaled vs. un-signaled threats (Martinon et al., 2019; Moaddab and Dabrowska, 2017), for review see (Olivera-Pasilio and Dabrowska, 2020).

On a cellular level, OT has shown robust modulatory influence on the inhibitory neurocircuitry of the hippocampus (Harden and Frazier, 2016; Maniezzi et al., 2019; Owen et al., 2013; Tirko et al., 2018), auditory cortex (Marlin et al., 2015), ventral tegmental area, VTA, (Hung et al., 2017; Xiao et al., 2017), lateral amygdala (Crane et al., 2020), and the CeA (Huber et al., 2005; Knobloch et al., 2012; Terburg et al., 2018; Viviani et al., 2011). Notably, although the BNST has one of the highest expression levels of OTR in the rodent brain (Dabrowska et al., 2011; Dumais et al., 2013; Tribollet et al., 1992; Veinante and Freund-Mercier, 1997) and receives OT inputs from hypothalamic nuclei (Dabrowska et al., 2011; Knobloch et al., 2012; Martinon et al., 2019), the effects of OT on excitability and synaptic transmission of BNST neurons remain elusive. Studies in the 90's from the Ingram group using electrophysiological approaches have shown that OT increases the spontaneous firing frequency in a subpopulation

of BNST neurons in lactating female rats (Ingram et al., 1990; Ingram and Moos, 1992; Wilson et al., 2005), but their type was not known.

$BNST_{DL}$ neurons are GABA-ergic (Cullinan et al., 1993; Dabrowska et al., 2013a; Sun and Cassell, 1993), and functionally interconnected via a dense intrinsic inhibitory network (Xu et al., 2016). As originally described by Rainnie and colleagues, $BNST_{DL}$ neurons can be classified into three major neuron types (I-III) based on their electrophysiological phenotype defined as a unique pattern of voltage deflection in response to transient depolarizing and hyperpolarizing current injections (Daniel et al., 2017; Hammack et al., 2007) and/or based on a single-cell mRNA expression of ion channel subunits (Hazra et al., 2011). Recently, it was shown that both Type II and Type III are output neurons of the $BNST_{DL}$, with major projections to the CeA (mainly Type II neurons), lateral hypothalamus (LH), and the VTA (mainly Type III neurons) (Yamauchi et al., 2018).

In the current study, using *in vitro* slice patch-clamp recordings in a whole-cell and cell-attached mode, we investigated the effects of OT on intrinsic excitability, inhibitory synaptic transmission and spontaneous firing in Type I-III $BNST_{DL}$ neurons in male Sprague-Dawley rats. We show that OT is a powerful modulator of the intrinsic inhibitory network such as it selectively increases the intrinsic excitability and the frequency of spontaneous firing of regular spiking, Type I neurons, which leads to increased inhibitory synaptic transmission (spontaneous Inhibitory Postsynaptic Currents, sIPSCs) and reduced spontaneous firing rate of Type II $BNST_{DL}$ neurons. We also combined injections of a fluorescent retrograde tracer into the CeA with electrophysiological recordings from fluorescent $BNST_{DL}$ neurons and we confirm that all recorded CeA-projecting neurons (BNST→CeA) are Type II neurons. Notably, we show that OT increases the sIPSCs frequency in these Type II BNST→CeA projection neurons. Finally, we demonstrate that OT reduces the amplitude of both spontaneous and evoked IPSCs selectively in Type III neurons via an OTR-dependent, postsynaptic mechanism. These results

demonstrate that OT directly excites Type I $BNST_{DL}$ interneurons, whereas it indirectly inhibits the Type II BNST→CeA projection neurons.

2. Material and methods

2.1. Animals

Male Sprague-Dawley rats (Envigo, Chicago, IL; 240-300 g) were housed in groups of three on a 12 h light/dark cycle (light 7 a.m. to 7 p.m.) with free access to water and food. Rats were habituated to this environment for one week before the experiments began. Experiments were performed in accordance with the guidelines of the NIH and approved by the Animal Care and Use Committee at RFUMS. A total of 153 rats were used for the experiments. The effects of OT on membrane properties were tested in 14 Type I neurons (from 10 rats), 13 Type II (12 rats), and 9 Type III neurons (8 rats). The effect of OT on evoked firing was tested on 12 Type I (11 rats), 8 Type II (7 rats), and 9 Type III neurons (8 rats). The effect of OT on the spontaneous firing was tested in 9 Type I (8 rats) and 19 Type II (16 rats). To study the effect of OT on sIPSCs, we recorded 14 Type II (12 rats), 6 Type I (5 rats), and 8 Type III neurons (8 rats). We recorded 6 Type II neurons (4 rats) in experiment with OTR antagonist, and 6 Type II neurons (5 rats) in TTX experiment. The effect of OT on the evoked IPSCs was tested in 5 Type I (5 rats), 8 Type II (8 rats), and 6 Type III (5 rats) neurons. We recorded 5 Type III (4 rats) neurons in experiments with OTR antagonist and 6 Type III (4 rats) with GABA-B antagonist. We recorded 13 retrogradelly labeled Type II BNST→CeA neurons from 11 rats and we recorded sIPSCs after application of OT in 5 of these Type II BNST→CeA neurons (from 5 rats).

2.2. Slice preparation for electrophysiology

Rats were anaesthetized with Isoflurane USP (Patterson Veterinary, Greeley, CO, USA) before decapitation. Brains were quickly removed and coronal 300 μm slices containing the $BNST_{DL}$ were prepared in ice-cold cutting solution (saturated with 95% O_2/ 5% CO_2) containing in mM: NaCl 130, KCl 3.5, $NaHCO_3$ 30, KH_2PO_4 1.1, $CaCl_2 \cdot 2H_2O$ 1, D-glucose 10, $MgCl_2$ $6H_2O$ 6, Kynurenate 2, pH 7.4, 290-300 mOsm. The slices were prepared using a Leica vibratome

(VT1200; Leica, Wetzlar, Germany), then incubated for 1 hr at 34°C in the cutting solution and subsequently transferred to room temperature in artificial cerebrospinal fluid (aCSF) containing in mM: NaCl 130, KCl 3.5, $NaHCO_3$ 30, KH_2PO_4 1.1, $CaCl_2 \cdot 2H_2O$ 2.5, D-glucose 10, and $MgCl_2 \cdot 6H_2O$ 1.3, Ascorbate 0.4, Thiourea 0.8, Na Pyruvate 2, pH 7.4, with osmolarity of 290-300 mOsm, continuously oxygenated with 95% O_2/ 5% CO_2. Next, the slices were transferred to a submerged recording chamber and perfused with aCSF at 33°C ± 1°C saturated with 95% O_2/ 5% CO_2 at a flow rate of 2-3 ml/min. $BNST_{DL}$ neurons were visualized using infrared differential interference contrast (IR-DIC) optic with an Upright microscope (Scientifica SliceScope Pro 1000, Clarksburg, NJ, USA).

2.3. Patch-clamp recordings

Whole-cell patch-clamp recordings were performed from $BNST_{DL}$ neurons, primarily in the oval nucleus of the BNST ($BNST_{OV}$), using glass pipette (4-8 MΩ) pulled from thick-walled borosilicate glass capillaries with a micropipette puller (Model P-97; Sutter Instrument, Novato, CA, USA) as before (Dabrowska et al., 2013b; Francesconi et al., 2009). To study the effects of OT (0.2 μM concentration based on (Crane et al., 2020; Xiao et al., 2017), oxytocin acetate salt, # H-2510, Bachem, Switzerland) on intrinsic membrane properties and firing activity the patch pipettes were filled with potassium gluconate internal solution containing in mM: K-gluconate 135, KCl 2, $MgCl_2 \cdot 6H_2O$ 3, HEPES 10, Na-phosphocreatine 5, ATP-K 2, GTP-Na 0.2, pH 7.3 adjusted with KOH, 300-305 mOsm. Intrinsic membrane properties experiments were performed in a presence of synaptic transmission blockers: the AMPA receptor antagonist CNQX (10 μM), the NMDA receptor antagonist AP-5 (50 μM), and GABA-A receptor antagonist, picrotoxin (25 μM). To study the effects of OT on the spontaneous inhibitory postsynaptic currents (sIPSCs), the patch pipettes were filled with high chloride internal solution in mM: KOH 110, $MgCl_2 \cdot 6H_2O$ 2, KCl 50, EGTA 0.2, ATP-Na 2, GTP-Na 0.3, HEPES 10, and Spermine 0.1, the pH was adjusted to 7.3 with D-gluconic acid and osmolarity was 300-305 mOsm. The evoked IPSCs (eIPCSs) were recorded with pipettes filled with K-gluconate solution as described above. In

order to isolate GABAergic eIPSCs, the eIPSCs were recorded at the holding voltage (Vh) of +10 mV, which is the reversal potential for the excitatory postsynaptic current. A stimulating pipette filled with aCSF was placed in the Stria Terminalis. For each neuron recorded the stimulus intensity was adjusted to give an eIPSCs of about 1/3 of the maximal amplitude and maintained throughout the experiment. We applied 10 paired pulse stimuli (ISI 50 msec) at the frequency of 0.2 Hz. The peak amplitude of the eIPSC was measured from the averaged responses. The responses were acquired each minute for 10 min before and 12 min after OT application. The paired pulse stimulus (50 ms ISI) was used to calculate the paired pulse ratio (PPR) between the mean amplitude of the second eIPSC divided by the amplitude of the first eIPSC. Here we used the PPR to evaluate a possible presynaptic mechanism of the OT effect on the BNST neurons inhibitory synaptic responses. To further examine a possible presynaptic mechanism due to an activation of presynaptic GABA-B receptors, in a subset of experiments we applied a specific GABA-B receptor antagonist CGP 55845 (2 μM) before OT.

To verify that the effects of OT were mediated by OTRs, selective and potent OTR antagonist d(CH2)5(1), D-Tyr(2), Thr(4), Orn(8), des-Gly-NH2(9)]-Vasotocin trifluoroacetate salt (Manning et al., 2012) (0.4 μM, OTA, V-905 NIMH Chemical Repository) was applied 10 min before OT in all whole-cell experiments. Recordings were performed with a Multiclamp 700B amplifier (Molecular Device, Sunnyvale, CA, USA). Current-clamp and voltage-clamp signals were acquired at 10 kHz with a 16-bit input-output board NI USB-6251 (National Instruments, Austin, TX) using custom MatLab scripts (Math-Work, Natick, MA) written by Dr. Niraj Desai (Desai et al., 2017). All neurons included in the analysis had a seal resistance > 1GΩ and an initial access resistance < 20 MΩ maintained for the entire recording period. Any cells showing a 10% change in the serial resistance were not included in the analysis.

2.3.1. Electrophysiological characterization of $BNST_{DL}$ neurons

At the beginning of the recording sessions in current clamp mode, neurons were electrophysiologically characterized into three types (Type I-III) using current pulses (450 msec

in duration) from -350 pA to 80 pA in 5 or 10 pA increments. Based on their characteristic voltage responses (Hammack et al., 2007), three types of neurons were identified in the $BNST_{DL}$. Type I neurons are regular firing and display spike frequency adaptation. These neurons also display moderate voltage sag that indicates the presence of the hyperpolarization-activated cation current (I_h). As a distinguishing feature of Type II neurons, post-inhibitory spikes are produced in response to preceding negative current steps that are related to the action of the low-threshold Ca^{2+} current. Additionally, Type II neurons display strong voltage sags under hyperpolarizing current pulses that indicate a high level of I_h current. Type III neurons differ from the previous two types in several aspects: they exhibit high rheobase and no voltage sag under negative current steps; they display prominent inward rectification that is caused by the activation of the inward rectifying K^+ current (I_{KIR}) at membrane potentials more negative than approximately −50 mV; and start firing after a characteristic slow voltage ramp mediated by the K^+ delayed current (I_D).

2.3.2. Cell-attached recordings

The spontaneous firing activity of Type I and II $BNST_{DL}$ neurons was recorded in a cell-attached voltage-clamp mode, using patch pipettes filled with K-gluconate solution as described above, without blockers of the synaptic transmission. To avoid a possible effect of amplifier-generated currents on the spontaneous firing activity during the recording the command potential was carefully adjusted at the value at which no current was flowing from the amplifier through the cell membrane as described before (Perkins, 2006). At the end of the spontaneous firing recording period, a gentle negative pressure was applied to break through the membrane into whole cell configuration and determine the neuron type in a current-clamp mode as described above.

2.3.3. The effect of OT on intrinsic membrane properties and spontaneous firing of Type I-III $BNST_{DL}$ neurons

We investigated the effects of OT on intrinsic membrane properties: resting membrane potential (RMP), input resistance (Rin), rheobase (Rh), threshold of the first action potential (Th)

(calculated as the voltage at which the depolarization rate exceeded 5 mV/ms), and latency of the first spike (Lat) evoked at the Rh current. We also investigated spiking ability by measuring the input-output (I-O) relationship before and after OT application. The steady state frequency (SSF) was measured by applying depolarizing pulses (1 sec in duration) of different amplitudes (0-80 pA in 10 pA increments). The SSF was determined as the average of the inverse of the inter-spike intervals (ISI) from all action potentials starting from the second action potential. The I/O curve was built before (pre), during, and after OT application (post).

A variety of afterhyperpolarizations (AHPs) following a single or a train of action potentials have been described to regulate the neuron excitability and spike frequency adaptation (Gu et al., 2008; Lopez de Armentia and Sah, 2004). They come in a temporal sequence of three AHPs: the fast AHP (fAHP) lasting 1-5 msec, the medium AHP (mAHP) lasting 50-200 msec, which is responsible for early spike frequency adaptation during a train of action potentials, and the late AHP (lAHP) lasting several seconds after a train of action potentials (Gu et al., 2005a). We investigated the effect of the OT on the amplitude of fAHP, mAHP and lAHP in all types of the $BNST_{DL}$ neurons. The amplitudes of the fAHP and mAHP following the first action potential evoked at Rh were calculated as the difference from the action potential threshold to the membrane voltage measured after 2-5 msec and 50-100 msec, respectively. The lAHP was measured at 2000 msec after the end of the depolarizing pulse, following generation of five action potentials. As the K^+ currents underlying these AHPs are considered to regulate spike frequency adaptation (Gu et al., 2008; Lopez de Armentia and Sah, 2004), we measured early and late spike frequency adaptation before and after OT application using a depolarizing pulse of 1 sec. We measured the instantaneous frequency for every action potential interval. The ISI number is the inter-stimulus interval between two consecutive action potentials. We measured the spike frequency adaptation rather than the spike frequency, because the firing of the BNST neurons, as described by Paré and colleagues (Rodríguez-Sierra et al., 2013), is adapting and not regular. This is a characteristic of all types of $BNST_{DL}$ neurons, including Type I (described as regular firing), which also adapt on a long current pulse.

We also performed recordings in cell-attached mode in Type I-II neurons and measured the spontaneous firing frequency before and after OT. The spontaneous firing frequency (Hz) was determined as the number of spontaneous spikes for every minute of recording.

2.3.4. The effect of OT on inhibitory synaptic activity of Type I-III $BNST_{DL}$ neurons

To study the effect of OT on spontaneous inhibitory postsynaptic currents (sIPSCs), the events were recorded from Type I-III neurons in a voltage clamp mode at holding potential of -70 mV. To isolate the sIPSCs, the recordings were made in the presence of the AMPA receptor antagonist CNQX (10 μM) and the NMDA receptor antagonist AP-5 (50 μM). The sIPSCs were characterized by their mean frequency, amplitude, and charge (calculated as the area under the curve) using custom scripts in MatLab. To reach an adequate number of events, the sIPSCs were acquired continuously in 2-minute sweeps during the entire recording time. The sIPSCs were recorded for 10 min in aCSF, followed by 12 min bath application of OT and followed by the drug washout (at least 10 more min after the OT application was completed). As sIPSCs are a combination of spike-independent IPSCs and spike-driven IPSCs, in some experiments the action potential generation was blocked with Tetrodotoxin (TTX, 1 μM, #1078; Tocris Bioscience, UK), leaving only the spike-independent IPSCs (miniature IPSCs, mIPSCs). $GABA_A$ receptor antagonist, picrotoxin (25 μM), was used at the end of the recordings to verify the GABA-ergic origin of the sIPSCs. Finally, to study the effect of OT on the evoked inhibitory synaptic transmission in Type I-III neurons, we recorded the eIPSCs by electrical stimulation of the Stria Terminalis.

2.3.5. CeA-projecting $BNST_{DL}$ neurons

To determine an electrophysiological phenotype of BNST→CeA neurons, rats were first bilaterally injected into the CeA with a retrograde tracer, green microbeads (Lumafluor Inc., 100 nl; from Bregma: AP: -2.8 mm, ML: +4.0 mm, DV: -7.9 mm), and were allowed to recover for 4-7 days before electrophysiological recordings. Stereotaxic surgeries were performed as before (Martinon et al., 2019; Moaddab and Dabrowska, 2017). The slices were illuminated with

CoolLED pE-300lite (Scientifica Ltd., Uckfield, UK) and ET - EGFP (FITC/Cy2) filter (Chroma Technology Corp, Bellows Falls, VT, US) to enable visually guided patching of fluorescent neurons. In a subset of these experiments we recorded sIPSCs from the fluorescent BNST→CeA neurons after application of OT as above. Slices were stored in 10% stabilized formalin post-recordings, mounted with Krystalon Mounting medium (Millipore Sigma, #64969-71), and analyzed with Nikon Eclipse E600 microscope (Melville, NY, US) and Olympus Fv10i confocal microscope for high magnification imaging (Center Valley, PA, US). Brain sections containing the CeA were also analyzed for the microbeads injection site. CeA was visualized with immunofluorescence using primary rabbit anti-enkephalin antibody (RA14124, Neuromics, MS, US) and secondary anti-rabbit Alexa Fluor 568 antibody (Life technologies Corporation, NY, US) according to the protocol as before (Dabrowska et al., 2013b).

2.4. Statistical analysis

Data are presented as MEAN ± standard error of mean (SEM). Data in line graphs are shown as the individual values from all recorded neurons (gray lines) as well as MEAN values (thick black line). Distribution of data sets was first evaluated with Kolmogorov-Smirnov test. Based on the normal distribution, the effects of OT on the sIPSCs, excitability, and firing frequency were analyzed by a repeated measures (RM) one-way analysis of variance (ANOVA) or mixed effects model, or paired *t*-tests, when applicable. Where the F-ratio was significant, all-pairwise post hoc comparisons were made using Tukey's or Sidak's tests. The statistical analyses were completed using GraphPad Prism version 9.0.0 (GraphPad Software Inc., San Diego, CA). $P < 0.05$ was considered significant.

3. Results

3.1. The effects of OT on intrinsic membrane properties and spontaneous firing in Type I-III $BNST_{DL}$ neurons.

In Type I neurons, OT induced a significant depolarization of RMP from -62.39 ± 0.84 mV to -57.94 ± 1.39 mV ($P = 0.0002$, $F(1.593, 19.12) = 15.76$, n = 14, mixed-effect analysis) in

comparison to baseline (pre, P = 0.0013) and washout (post, P = 0.0304, **Fig. 1A-B**). This was associated with a significant increase of Rin from 170.98 ± 8.6 MΩ to 233.64 ± 18.6 MΩ (P = 0.0085, n = 9, paired *t*-test, **Fig. 1C**). As a consequence, OT induced a significant reduction of Rh from 21.96 ± 2.29 pA to 17.32 ± 2.26 pA (P = 0.0457, F (1.341, 16.09) = 4.226, n = 14, mixed-effect analysis) in comparison to baseline (pre, P = 0.0023, **Fig. 1D**). The Th of the first spike was also significantly reduced from - 38.38 ± 0.68 mV to -39.75 ± 0.88 mV after OT (P = 0.0164, F (1.472, 20.61) = 5.749), in comparison to baseline (pre, P = 0.0346**, Fig. 1E**). When the OTR antagonist (OTA) was applied for 10 min before and during OT application, OT did not significantly affect RMP (P = 0.0710), Rh (P = 0.1231), Th (P = 0.3532) or Lat (P = 0.6252, **not shown**). In contrast to Type I neurons, OT did not affect the intrinsic membrane properties of Type II and III neurons (**Table 1**).

In addition, OT caused a leftward shift of input/output (I-O) relationship in Type I neurons, demonstrating a significant increment effect on SSF at 40 pA (P = 0.0024, F (1.667, 15.01) = 10.11, n = 12), at 50 pA (P = 0.0271, F (1.863, 16.76) = 4.628, n = 11), and at 60 pA (P = 0.0271, F (1.688, 11.82) = 5.267, mixed-effects analysis, n = 10). Post-hoc test showed a significant increase of the SSF after OT from 6.81 ± 0.68 Hz to 8.96 ± 0.63 Hz in comparison to baseline (pre, P = 0.0032) and washout (post, P = 0.0095) at 40 pA; from 8.73 ± 0.73 Hz to 11.20 ± 0.70 Hz (P = 0.0163, pre and P = 0.0226, post) at 50 pA; and from 9.22 ± 0.57 Hz to 11.89 ± 0.99 Hz (P = 0.0271, pre and P = 0.0054, post) at 60 pA. The OT effect reached a trend at 30 pA (from 5.64 ± 0.5 Hz to 7.31 ± 0.53 Hz, P = 0.0820) and at 70 pA (from 10.79 ± 0.6 Hz to 13.62 ± 0.99 Hz, P = 0.0794). The effect was not significant at 20 pA (P = 0.1268) and 80 pA (P = 0.1320, **Fig. 2A-B**). Importantly, in the presence of OTA, OT did not affect the SSF of Type I neurons at 80 pA (P = 0.7960), 70 pA (P = 0.4237), 60 pA (P = 0.6312), 50 pA (P = 0.4299), 40 pA (P = 0.3365), or 30 pA (P = 0.4817, **Fig. 2C**). OT did not affect SSF in Type II (F (1, 7) = 0.0020, P = 0.9652) or Type III neurons (F (1, 8) = 2.907, P = 0.1266, **Fig. 2D-E**).

Figure 1

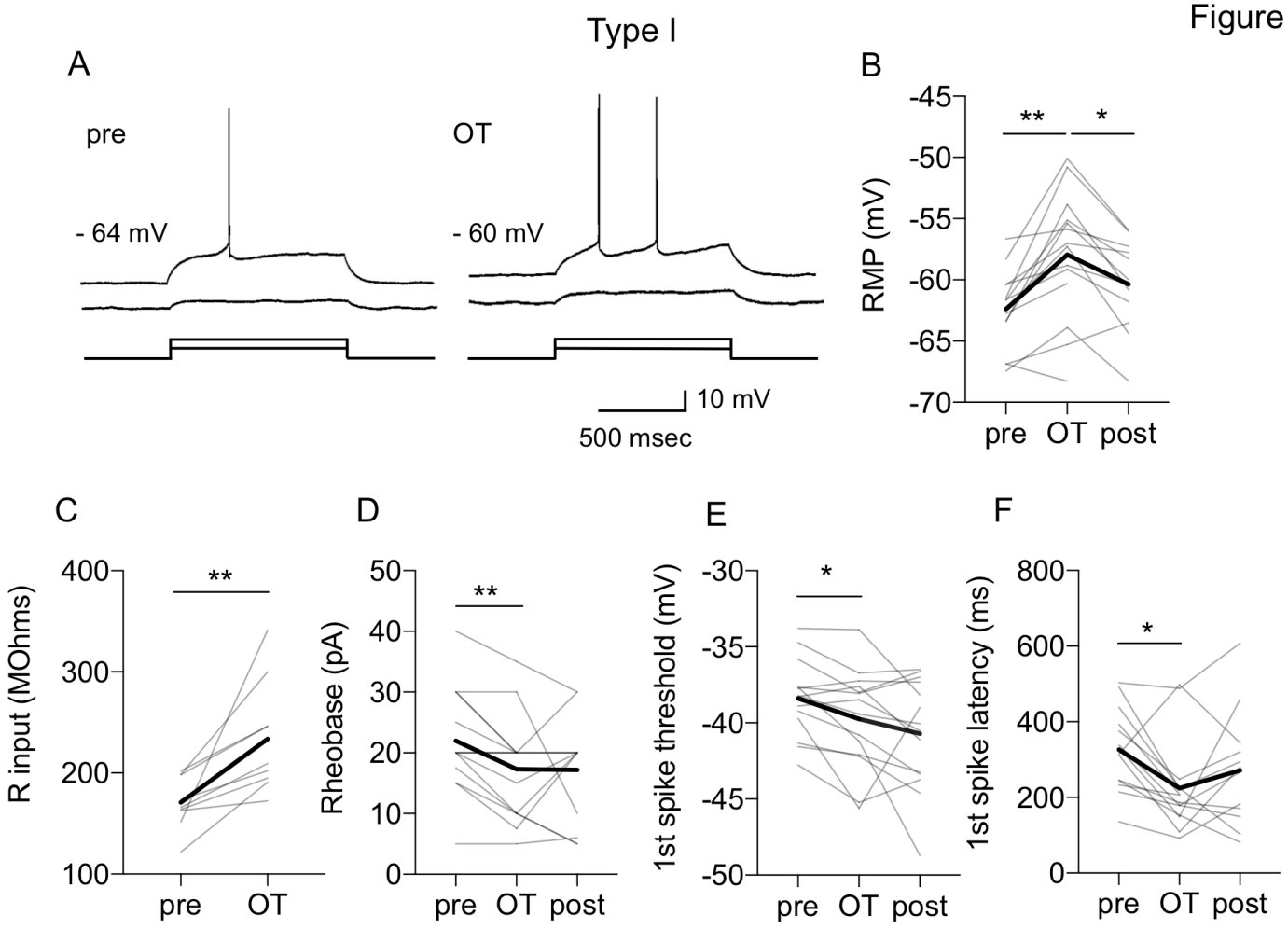
Type I
A
pre
- 64 mV
OT
- 60 mV
10 mV
500 msec
B
RMP (mV)
-45
-50
-55
-60
-65
-70
**
*
pre
OT
post
C
R input (MOhms)
400
300
200
100
**
pre
OT
D
Rheobase (pA)
50
40
30
20
10
0
**
pre
OT
post
E
1st spike threshold (mV)
-30
-35
-40
-45
-50
*
pre
OT
post
F
1st spike latency (ms)
800
600
400
200
0
*
pre
OT
post

Type I neurons	Pre	OT
RMP (mV)	-62.39 ± 0.84	**57.94 ± 1.39 ****
Rin (MOhms)	170.98 ± 8.6	**233.64 ± 18.6 ***
Rh (pA)	21.96 ± 2.29	**17.32 ± 2.26 ****
Th (mV)	-38.38 ± 0.68	**39.75 ± 0.88 ***
Lat (ms)	326.44 ± 28.63	**224.58 ± 32.51 ****
fAHP (mV)	8.63 ± 0.89	**7.47 ± 0.77 ****
mAHP (mV)	10.69 ± 0.61	**8.45 ± 0.72 ******
lAHP (mV)	0.49 ± 0.12	0.41 ± 0.1
Type II neurons		
RMP (mV)	-57.04 ± 0.86	-56.74 ± 0.78
Rin (MOhms)	221.8 ± 29.27	276.03 ± 46.66
Rh (pA)	16.92 ± 2.52	15 ± 2.66
Th (mV)	-39.87 ± 0.95	-40.32 ± 1.05
mAHP (mV)	10.96 ± 0.83	10.79 ± 0.86
lAHP (mV)	1.58 ± 0.33	1.41 ± 0.39
Type III neurons		
RMP (mV)	-65.73 ± 1.42	-63.3 ± 1.83
Rin (MOhms)	120.66 ± 23.12	156.93 ± 29.7
Rh (pA)	56.46 ± 8.92	48.33 ± 7.36
Th (mV)	-37.28 ± 0.85	-37.08 ± 0.93
mAHP (mV)	8.68 ± 0.62	7.07 ± 0.93
lAHP (mV)	0.26 ± 0.12	0.22 ± 0.04

Table 1. Intrinsic membrane properties and firing activity of Type I-III $BNST_{DL}$ neurons after OT (0.2 μM) application respective to baseline (pre-OT). *****P* < 0.0001, ***P* < 0.01, **P* < 0.05. In Type II neurons OT did not affect RMP (*P* = 0.0985), Rin (*P* = 0.1377), Rh (*P* = 0.0964), Th (*P* = 0.5027), mAHP (*P* = 0.9147) or lAHP (*P* = 0.6340). Similarly, in Type III neurons OT did not significantly change RMP (*P* = 0.1066), Rin (*P* = 0.0788), Rh (*P* = 0.1664), Th (*P* = 0.5150), mAHP (*P* = 0.0775) or lAHP (*P* = 0.6472).

Figure 2

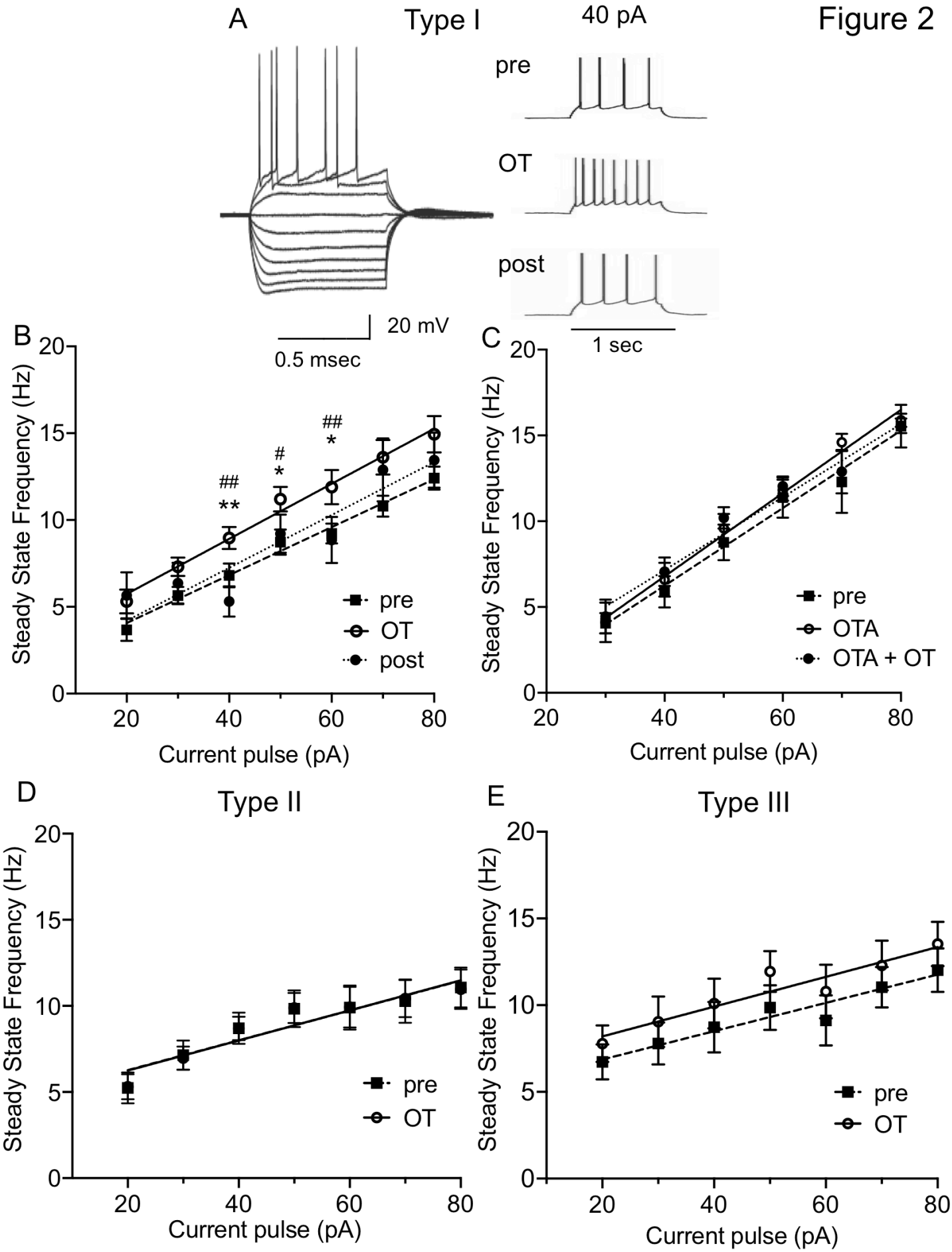
A
Type I
40 pA
pre
OT
post
20 mV
0.5 msec
1 sec
B
Steady State Frequency (Hz)
Current pulse (pA)
##
**
#
*
##
*
pre
OT
post
C
Steady State Frequency (Hz)
Current pulse (pA)
pre
OTA
OTA + OT
D
Type II
Steady State Frequency (Hz)
Current pulse (pA)
pre
OT
E
Type III
Steady State Frequency (Hz)
Current pulse (pA)
pre
OT

This increase in the spiking ability of Type I neurons after OT was associated with a significant shortening of the first spike's latency from 326.44 ± 28.63 msec to 224.58 ± 32.51 msec (*P* = 0.0185, F (1.971, 23.66) = 4.775, n = 14, mixed-effect analysis), in comparison to baseline (pre, *P* = 0.0083, **Fig. 1F**). We also investigated the effects of OT on the fAHP, the mAHP and the lAHP. In Type I neurons, OT significantly reduced the amplitude of fAHP (*P* = 0.0124, F (1.473, 17.68 = 6.493, mixed-effects analysis, n = 14), from 8.63 ± 0.89 mV to 7.47 ± 0.77 mV, *P* = 0.0062, in comparison to pre, **Fig. 3A-B**) and mAHP (*P* <0.0001, F (1.844, 22.13) = 23.25, mixed effect analysis, n = 14), from 10.69 ± 0.61 mV to 8.45 ± 0.72 mV (*P* = 0.0001 vs. pre, and *P* = 0.0003 vs. post), **Fig. 3A, D**). Notably, OT did not affect the amplitudes of fAHP (*P* = 0.2220, n = 7, **Fig. 3C**) and mAHP (*P* = 0.3968, n = 7, RM one way-ANOVA, **Fig. 3E**) in the presence of OTA. Lastly, OT did not significantly affect the amplitude of lAHP in Type I neurons (*P* = 0.2401, **Table 1**). In contrast to Type I neurons, OT did not affect the amplitude of mAHP and lAHP of Type II and III neurons (**Table 1**). We did not measure the effect of OT on fAHP in these neurons, because the fAHP is not present in Type II and Type III neurons.

We also investigated if these changes in AHP amplitude could modify the spike frequency adaptation. We found that OT significantly increased the instantaneous frequency of ISIs (*P* < 0.0001, F (1, 13) = 82.69, n = 13, mixed effects model) and post-hoc test showed a significant OT effect on frequency (in Hz) of ISI number 2 (ISI-2) from 16.77 ± 1.55 to 19.57 ± 1.2 (*P* = 0.0006), ISI-3 from 12.48 ± 0.88 to 16.19 ± 1.09 (*P* < 0.0001), ISI-4 from 11.92 ± 0.88 to 14.87 ± 0.76 (*P* = 0.0006), ISI-5 from 11.36 ± 0.68 to 14.58 ± 0.77 (*P* = 0.0001), ISI-6 from 11.26 ± 0.72 to 13.93 ± 0.76 (*P* = 0.0079), and ISI-7 from 10.58 ± 0.64 to 13.44 ± 0.88 (*P* = 0.0051, **Fig. 3F**).

During cell-attached recordings, the spontaneous firing was present in 7 out of 9 Type I neurons and OT significantly increased the firing rate in the spontaneously firing neurons from 0.88 ± 0.66 Hz to 2.19 ± 0.93 Hz (*P* = 0.0242, paired *t*-test, **Fig. 4A-B**). In addition, although only 7 out of 19 recorded Type II neurons showed spontaneous firing in a cell-attached mode, in all spontaneously firing Type II neurons, OT significantly reduced the firing rate from 1.96 ± 0.63

Figure 3

Type I

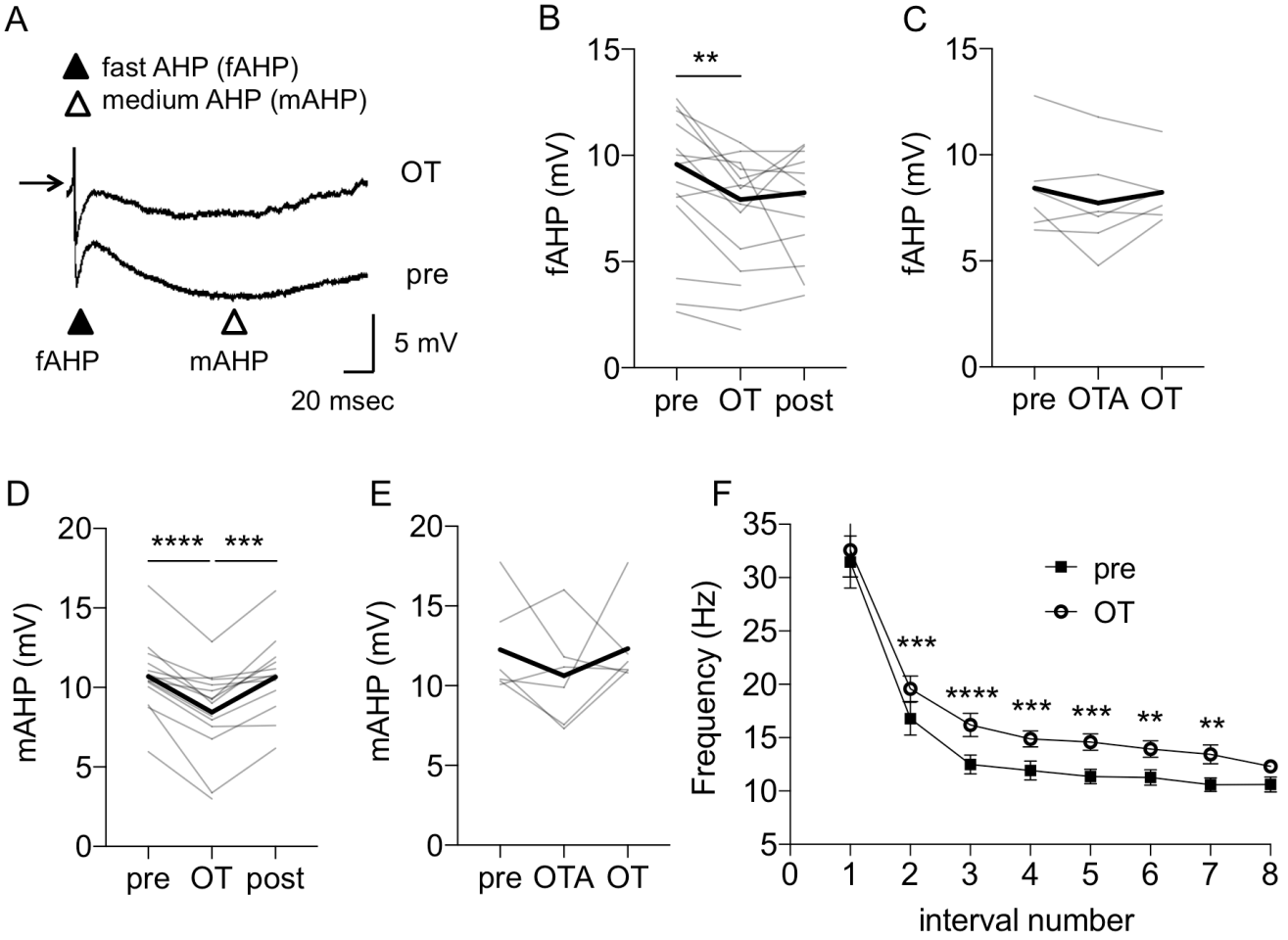

Figure 4

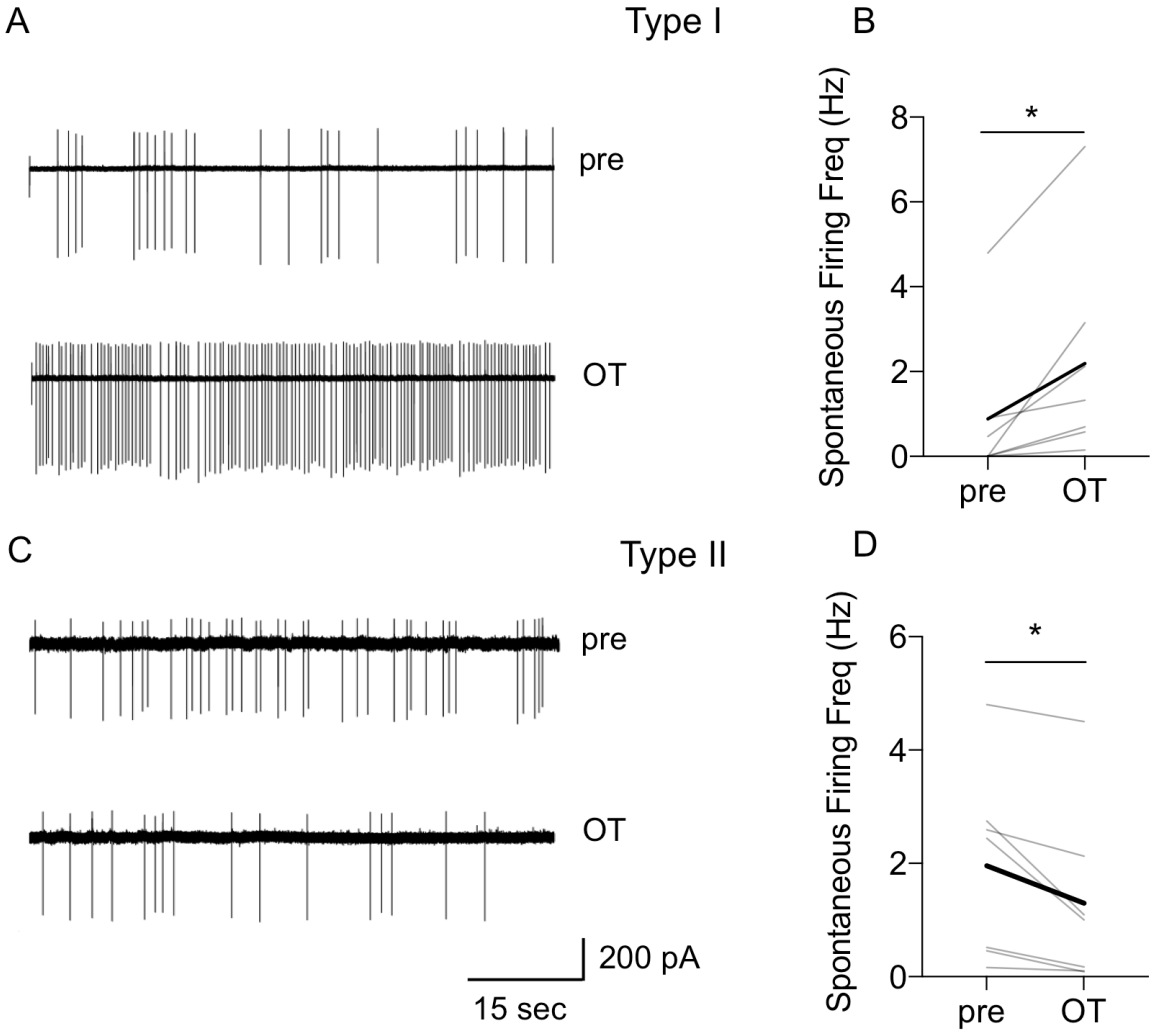
A
Type I
pre
OT
B
Spontaneous Firing Freq (Hz)
8
6
4
2
0
*
pre
OT
C
Type II
pre
OT
200 pA
15 sec
D
Spontaneous Firing Freq (Hz)
6
4
2
0
*
pre
OT

Hz to 1.29 ± 0.60 Hz, (*P* = 0.0304, paired *t*-test, n = 7, **Fig. 4C-D**). In addition, in Type II neurons recorded with high seal (>2GΩ), which did not fire spontaneously, we also estimated the effect of OT on the RMP by measuring the voltage in cell-attached current clamp mode as described before (Perkins, 2006) and we show that OT application does not change the RMP (pre 58.6 ± 2.52 mV to 58.5 ± 2.42 mV, n = 6).

Overall, these results suggest that OT increases the intrinsic excitability and facilitates the spontaneous firing selectively in Type I $BNST_{DL}$ neurons, whereas it reduces spontaneous firing rate in Type II $BNST_{DL}$ neurons.

3.2. The effects of OT on inhibitory synaptic transmission in Type I-III $BNST_{DL}$ neurons.

In Type I neurons, OT did not affect the sIPSCs frequency (*P* = 0.3018), amplitude (*P* = 0.3347), or total charge (*P* = 0.6087, n = 7, paired *t*-test, **not shown**). Moreover, OT did not change the amplitude of the eIPSC in Type I neurons (*P* = 0.2449, paired *t*-test, n = 5, **not shown**).

In Type II $BNST_{DL}$ neurons, application of OT caused a significant increase in the frequency of sIPSCs in 12 out of 14 recorded neurons (*P* = 0.0022, F (1.058, 12.17) = 14.41, n = 14, mixed-effect analysis) from 1.03 ± 0.20 Hz to 2.64 ± 0.47 Hz vs. baseline (pre, *P* = 0.0033), and vs. washout (post, *P* = 0.0018, **Fig. 5A-B**). Notably, the effect of OT on the sIPSCs frequency was not associated with a significant change in the amplitude (*P* = 0.5855, F (1.563, 17.19) = 0.4718, n = 14, mixed-effect analysis, **Fig. 5C**) or in the total charge (*P* = 0.5744, **not shown**). OT did not increase the sIPSCs frequency in the presence of OTA (*P* = 0.1788, F (1.469, 8.814) = 2.135, n = 6, RM ANOVA, **Fig. 5D**). In addition, when the spike-driven sIPSCs were blocked with TTX (*P* = 0.0151, F (1.030, 6.179) = 10.98, n = 6, RM ANOVA), OT no longer affected the frequency of miniature IPSCs (mIPSCs) of Type II neurons (*P* = 0.9975, **Fig. 5E**). Finally, OT did not affect the eIPSCs amplitude (at the Vh of +10 mV) in Type II neurons, from 266.76 ± 55.43 pA (pre) to 316.17 ± 82.49 pA (post, *P* = 0.2459, paired *t*-test) (**Fig. 6A** and **6C**).

Figure 5

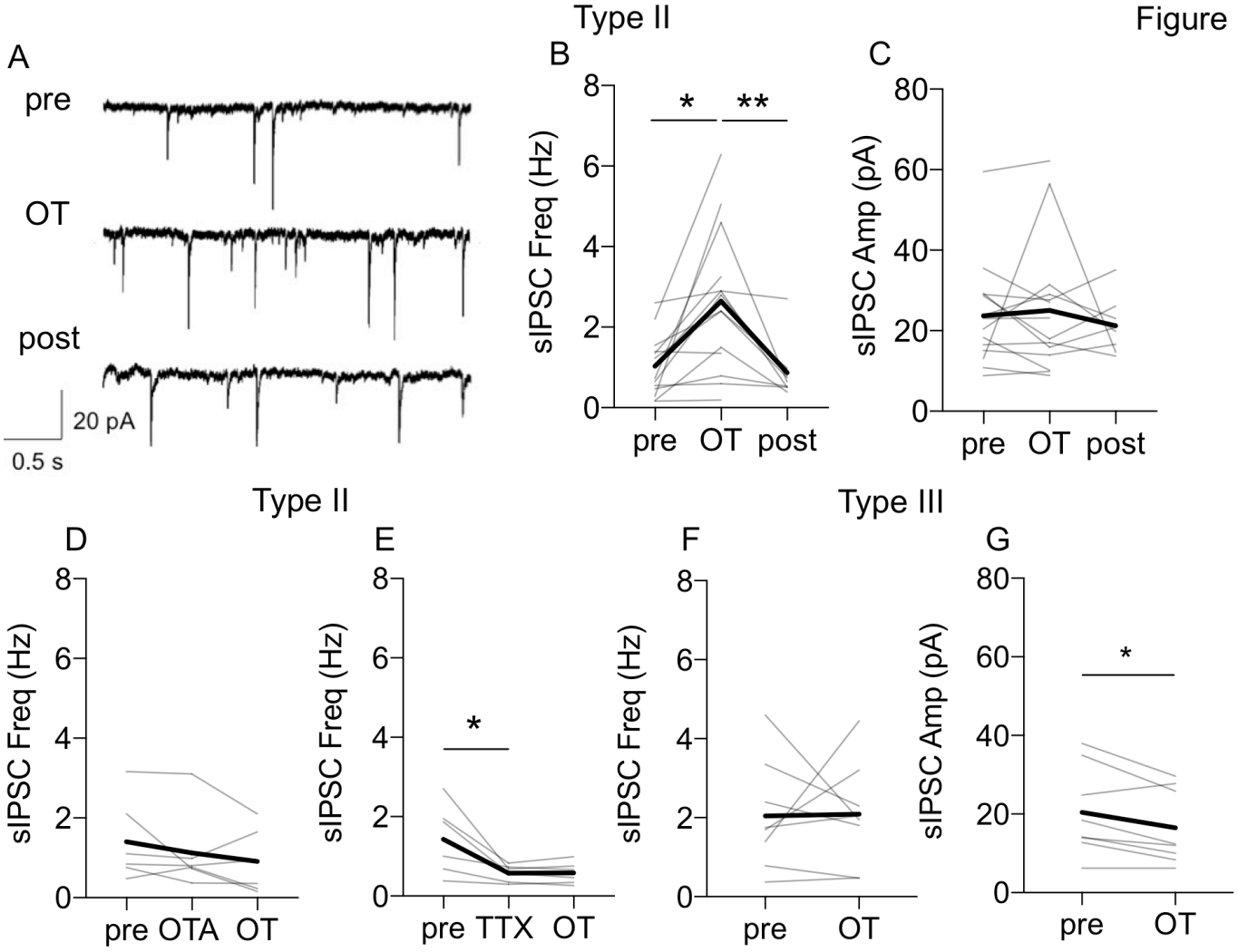
Type II
A
pre
OT
post
20 pA
0.5 s
B
sIPSC Freq (Hz)
*
**
pre
OT
post
C
sIPSC Amp (pA)
pre
OT
post
Type II
D
sIPSC Freq (Hz)
pre
OTA
OT
E
sIPSC Freq (Hz)
*
pre
TTX
OT
Type III
F
sIPSC Freq (Hz)
pre
OT
G
sIPSC Amp (pA)
*
pre
OT

These results demonstrate that OT indirectly increases the frequency of spike-driven sIPSCs in Type II neurons.

In Type III neurons, OT did not affect the frequency (*P* = 0.9440, **Fig. 5F**), but it reduced amplitude (*P* = 0.0314, **Fig. 5G**) and total charge of sIPSCs (*P* = 0.0372, paired *t*-test, n = 6, **not shown**). In addition, in Type III neurons, OT significantly reduced the amplitude of the eIPSCs from 286.76 ± 97.41 pA (pre) to 210.69 ± 78.57 pA (*P* = 0.0105, paired *t*-test, n = 6, **Fig. 6B** and **6D**). This reduction of the eIPSC amplitude was not associated with a significant change in the PPR (*P* = 0.5672, paired *t*-test, **Fig. 6E**). Notably, in a presence of OTR antagonist, OT did not reduce the amplitude of eIPSCs in Type III neurons (F (1.421, 7.105) = 0.1722, *P* = 0.7739, RM ANOVA, n = 6), **Fig. 6F**). However, OT significantly reduced the amplitude of the eIPSCs in the presence of the GABA-B receptor antagonist CGP 55845 from 282.45 ± 50.58 pA to 219.38 ± 55.83 pA (F (1.258, 6.291) = 11.16, *P* = 0.0122, RM ANOVA, n = 6, **Fig. 6G**), showing a significant reduction in comparison to pre *(P* = 0.0413), and post (*P* = 0.0374). Again, this reduction of the eIPSC amplitude after OT in the presence of CGP 55845 was not associated with a significant change in the PPR (F (1.438, 7.191) = 2.560, *P* = 0.1499, RM ANOVA, n = 6, **not shown**). Overall, these findings suggest that in Type III neurons OT affects the synaptic response through a postsynaptic mechanism.

3.3. CeA-projecting $BNST_{DL}$ neurons

In rats injected with microbeads into the CeA (**Fig. 7A**), retro-labeled fluorescent neurons were found in subdivisions of the $BNST_{DL}$, primarily in the oval nucleus of the $BNST_{DL}$ ($BNST_{OV}$) and to a lesser extent in anteromedial BNST ($BNST_{AM}$, **Fig. 7B-C**). We recorded 13 fluorescent neurons from 11 rats injected with microbeads to the CeA (**Fig. 7D**), and all 13-recorded neurons were classified as Type II (**Fig. 7E**). To determine OT effects in these Type II BNST→CeA neurons, we performed whole cell patch-clamp recordings in 5 of these Type II fluorescent neurons and we measured frequency and amplitude of sIPSCs before and after OT application. We demonstrate that OT increased the sIPSCs frequency (F (1.004, 4.016) = 10.99,

Figure 6

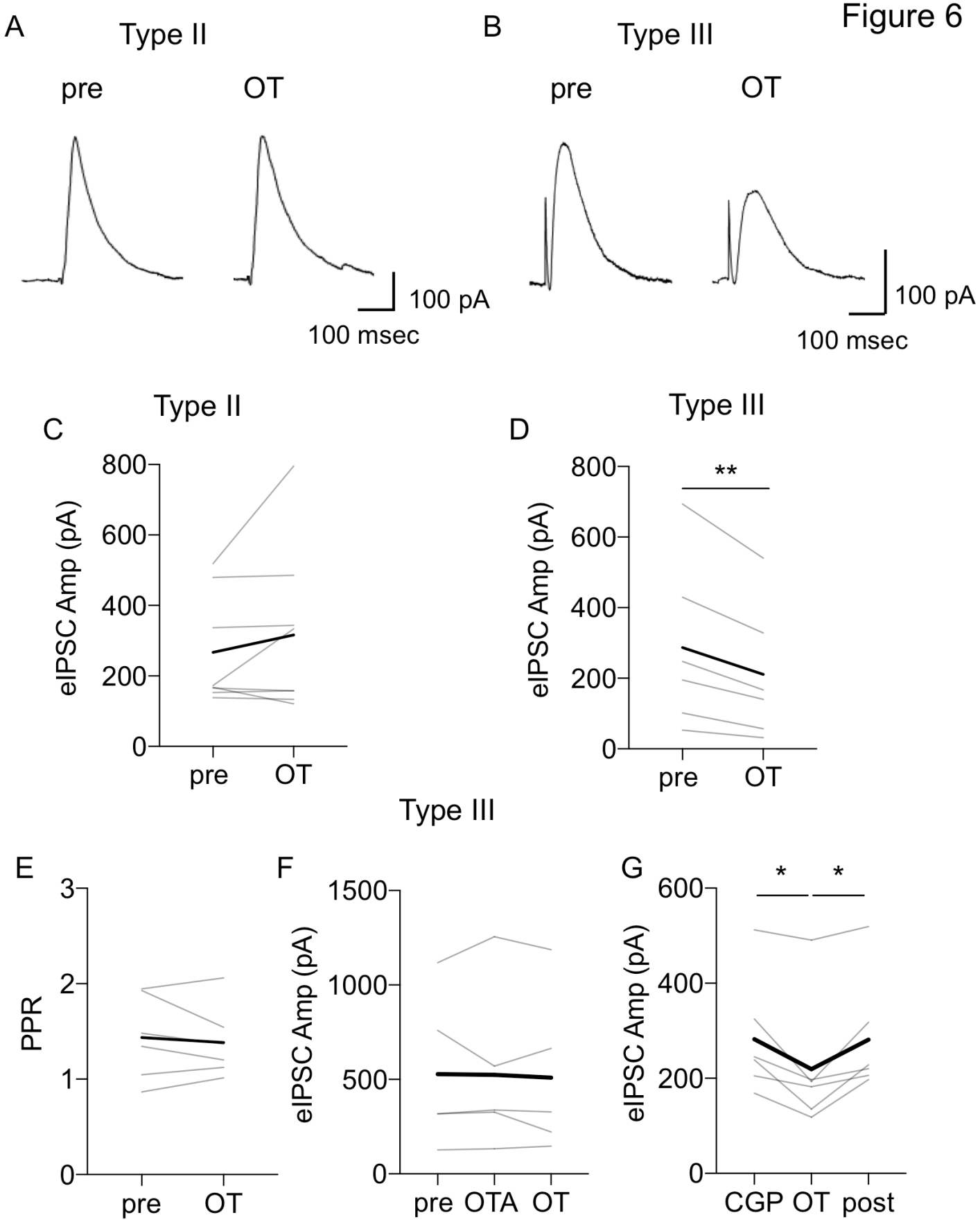
A
Type II
pre
OT
100 pA
100 msec
B
Type III
pre
OT
100 pA
100 msec
C
Type II
eIPSC Amp (pA)
800
600
400
200
0
pre
OT
D
Type III
**
eIPSC Amp (pA)
800
600
400
200
0
pre
OT
Type III
E
PPR
3
2
1
0
pre
OT
F
eIPSC Amp (pA)
1500
1000
500
0
pre
OTA
OT
G
*
*
eIPSC Amp (pA)
600
400
200
0
CGP
OT
post

Figure 7

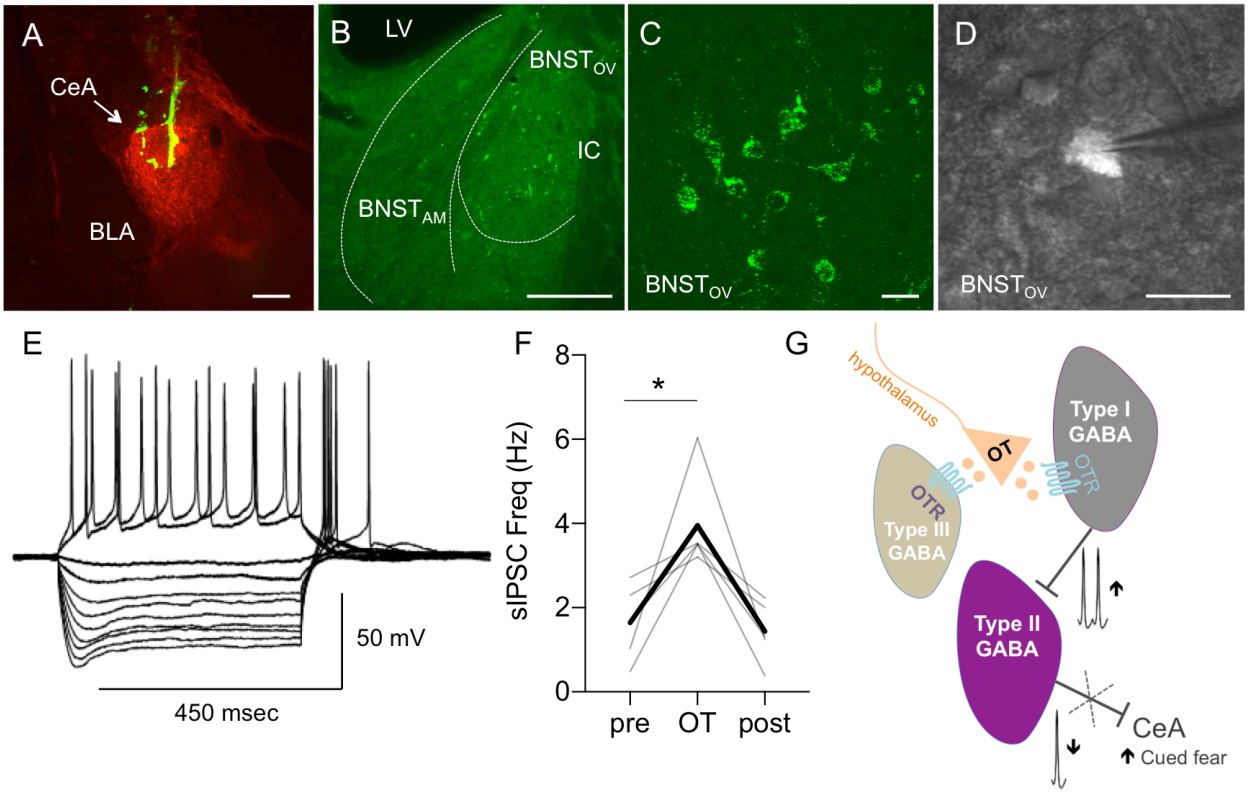
A
CeA
BLA
B
LV
BNST$_{OV}$
IC
BNST$_{AM}$
C
BNST$_{OV}$
D
BNST$_{OV}$
E
50 mV
450 msec
F
sIPSC Freq (Hz)
8
6
4
2
0
*
pre
OT
post
G
hypothalamus
OT
OTR
OTR
Type I GABA
Type III GABA
Type II GABA
CeA
Cued fear

P = 0.0293, RM ANOVA, n = 5) from 1.64 ± 0.41 Hz to 3.95 ± 0.52 Hz (vs. pre, *P* = 0.0416 (**Fig. 7F**), but not amplitude (F (1.007, 4.026) = 3.099, *P* = 0.1527, **not shown**) in the fluorescent Type II BNST→CeA neurons, showing that OT inhibits the Type II BNST→CeA output neurons (**Fig. 7G**).

4. Discussion

Here we demonstrate that OT regulates the intrinsic inhibitory network of the $BNST_{DL}$, where it increases intrinsic excitability and spontaneous firing of Type I, regular spiking interneurons, which leads to a potentiation of GABA-ergic inhibition and a reduction of spontaneous firing of Type II, burst firing neurons. Using visually guided patching of retro-labeled $BNST_{DL}$ neurons, we confirm that Type II are output neurons of the $BNST_{DL}$, which project to the CeA (BNST→CeA) and we show that OT inhibits these Type II BNST→CeA neurons. Furthermore, we show that OT reduces the spontaneous and evoked GABA-ergic inhibition in Type III $BNST_{DL}$ neurons, via a postsynaptic mechanism. Therefore, we demonstrate that there are three groups of OT-responsive neurons in the $BNST_{DL}$; a population of interneurons (Type I) that is directly excited by OTR activation, a group of BNST→CeA projection neurons (Type II), which are indirectly inhibited by OT, and a group of Type III neurons, which demonstrate reduced GABA-ergic inhibition after OT application (see **graphical abstract and Fig. 7G**). The OT-mediated inhibition of the BNST→CeA output neurons has powerful implications for the modulation of fear and anxiety-like behaviors.

Neurons of the $BNST_{DL}$ are GABA-ergic (Cullinan et al., 1993; Dabrowska et al., 2013a; Sun and Cassell, 1993), and can be categorized into three major types (I-III) (Daniel et al., 2017; Hammack et al., 2007). Type I neurons, characterized by regular firing and lack of burst-firing activity (Hammack et al., 2007; Hazra et al., 2011), were classified as interneurons by Paré and colleagues (Rodríguez-Sierra et al., 2013). This has been recently supported by retrograde labeling showing a very small fraction of Type I neurons (in comparison to Type II and Type III) projecting outside of the $BNST_{DL}$ (Yamauchi et al., 2018). We show that Type I

neurons are the primary OT-responsive neurons of the $BNST_{DL}$ as demonstrated by their increased excitability and spontaneous firing rate after OT application. Previous studies using single unit recordings showed that OT increased the spontaneous firing rate of 50% of BNST neurons in lactating female rats (Ingram et al., 1990), and the magnitude of the response was significantly potentiated during lactation (Ingram and Moos, 1992). Notably, in our study, the excitatory effects of OT in Type I neurons are paralleled by increased inhibitory transmission observed in Type II $BNST_{DL}$ neurons. The specific effect of OT on the sIPSCs frequency, but not amplitude, suggests a presynaptic mechanism in Type II neurons. In addition, since the effect was no longer observed when the spike-driven IPSCs were suppressed with TTX, this indicates an indirect influence driven by an increased spontaneous firing of $BNST_{DL}$ interneurons. This has been further supported by the lack of the OT effect on eIPSCs in Type II neurons, suggesting that the inhibitory effect of OT in Type II neurons is not a result of the stimulation of the extrinsic inhibitory projections via stria terminalis.

In contrast, in Type III neurons, OT reduces the amplitude and the total charge, but not the frequency of sIPSCs and eIPSCs, without changing the PPR. The effect of OT on eIPSCs was also observed in the presence of an antagonist for presynaptic GABA-B receptors, further excluding presynaptic effect. Overall, these results indicate a postsynaptic mechanism of OT in Type III neurons. OT was shown previously to reduce evoked GABA-ergic transmission in the CeA (Tunstall et al., 2019) and to depress GABA-ergic synapses in the supraoptic nucleus of the hypothalamus via postsynaptic increase of Ca^{2+} due to the activation of G-protein coupled receptors (Alger and Nicoll, 1980; Brussaard et al., 1996). However, since in our hands the effect on the amplitude was accompanied by a reduction in the total charge, this could potentially indicate shortening of GABA channel opening (Martina et al., 1994) via OTR-mediated increases in intracellular Ca^{2+}, as demonstrated after OTR activation before (Brussaard et al., 1996). Therefore, in Type III neurons OT might reduce the amplitude of sIPSCs and eIPSC through a postsynaptic mechanism involving signal transduction-mediated regulation of intracellular Ca^{2+} levels.

To further investigate the OT effects on intrinsic excitability and firing, we demonstrated that OT reduced fAHP and mAHP selectively in Type I neurons. AHPs generated after a single action potential or a train of action potentials limit the frequency of neuronal firing (Alger and Nicoll, 1980), as demonstrated by a significant increase in action potential firing after pharmacological inhibition of AHPs (Pedarzani and Storm, 1993). The fAHP, mediated by BK channels, is responsible for early spike frequency adaptation in many neuronal types (Gu et al., 2007). The mAHP is mediated by the non-inactivating M-current, which blockade with selective antagonist reduces late spike adaptation (Gu et al., 2008, 2005b). An OTR-mediated increase of neuronal excitability was recently shown in the hippocampus, where a selective OTR agonist induced membrane depolarization and increased membrane resistance in CA2 pyramidal cells leading to a leftward shift in their firing frequency-current relationship (Tirko et al., 2018). Here we show that OT-mediated excitation of Type I neurons in the $BNST_{DL}$ was associated with a significant increase in instantaneous frequency of action potentials due to the reduction in the early and late adaptation. Therefore, by acting on potassium conductances OT might increase the intrinsic excitability and the spontaneous firing of Type I neurons.

According to our knowledge, this is the first study utilizing cell-attached mode in a cell-type specific manner to show that in the $BNST_{DL}$, the majority of Type I neurons fire spontaneously, and this effect is further potentiated by OT. Notably, although we showed that the majority of Type II neurons remain silent even during cell-attached configuration, in all spontaneously firing Type II neurons, OT application reduced the rate of firing. Notably, the indirect inhibitory effect on spontaneous firing of Type II neurons was further confirmed by the lack of the OT effect on current-evoked firing in these neurons, which was investigated in a presence of synaptic transmission blockers. The latter further suggests that OT does not alter intrinsic properties of Type II neurons and instead, reduces the spontaneous firing rate and so their inhibitory synaptic transmission via the direct excitatory effect on Type I neurons.

The BNST was not entirely isolated during recordings, such as the slice also potentially contained GABA-ergic neurons in the medial preoptic area (Okamura et al., 1990), which express OTR (Sharma et al., 2019), and project to the BNST (Simerly and Swanson, 1988). However, this projection primarily targets the principal encapsulated nucleus in the posterior BNST (Maejima et al., 2015), where OTR are involved in reproductive behavior (Kremarik et al., 1991). Notably, the posterior BNST was not a part of our slice preparation. In addition, although we cannot entirely rule out a possibility that some inhibitory inputs to the $BNST_{DL}$ might be originating from anteromedial ($BNST_{AM}$) or ventral BNST ($BNST_{VEN}$), which were included in our slice, the intrinsic inhibitory projections in the BNST have been primarily shown to originate in the $BNST_{DL}$, mainly the $BNST_{OV}$, and target $BNST_{AM}$ and $BNST_{VEN}$, whereas opposite projections are rare (Gungor and Paré, 2016). Therefore, our results strongly suggest that Type I neurons are $BNST_{DL}$ interneurons providing inhibitory synaptic input to Type II neurons, an effect potentiated by OT.

It is important to note that the BNST also contains neurons producing arginine-vasopressin (AVP) (al-Shamma and De Vries, 1996) and has a high expression of AVP receptors, V1AR (Grundwald et al., 2016). As OT shows a relatively high affinity toward V1AR, this raises a possibility of non-specific effects via V1AR. However, all the significant OT effects in our study were blocked by OTA, which is highly selective toward OTR with a negligible affinity toward V1AR, see (Manning et al., 2012).

Similar modulation of the intrinsic inhibitory network by OT was shown in a variety of limbic brain regions, including the CeA. The CeA and the BNST share many similarities, including predominantly GABA-ergic nature, analogous peptidergic cell types, as well as similar intrinsic and extrinsic connectivity, and together they form an extended amygdala complex (Alheid, 2003; Sun and Cassell, 1993). Interestingly, in the CeA, there are two groups of OT-responsive neurons. A group of interneurons located in the lateral nucleus of the CeA (CeL) (Gozzi et al., 2010) is excited by OTR activation (Huber et al., 2005; Terburg et al., 2018; Viviani

et al., 2011), which strengthens inhibitory input to medial nucleus of the CeA (CeM) output neurons, which were shown to projecting to lateral periaqueductal gray and reduce contextual fear (Viviani et al., 2011), for review see (Beyeler and Dabrowska, 2020). Similarly to the effects we observed in the $BNST_{DL}$, OTR-mediated indirect inhibition of the CeM output neurons was demonstrated as increased frequency of sIPSC during whole-cell recordings and reduced spontaneous firing rate in a cell-attached configuration. Similarly, in the hippocampus (Harden and Frazier, 2016; Maniezzi et al., 2019; Owen et al., 2013; Tirko et al., 2018; Zaninetti and Raggenbass, 2000), lateral amygdala (Crane et al., 2020), and the prefrontal cortex (Marlin et al., 2015; Nakajima et al., 2014), OT was shown to excite a population of interneurons, including fast-spiking parvalbumin interneurons, which were shown to inhibit glutamatergic projection neurons.

We show that in the $BNST_{DL}$ OT inhibits Type II neurons, whereas it reduces the evoked inhibition on Type III neurons. Recently, both Type II and Type III were demonstrated output neurons of the $BNST_{DL}$, with major projections to the CeA (62% of Type II and 33% of Type III), LH (83% of Type III), and the VTA (17% of Type II, 79% of Type III neurons). In our experiments, all the retrogradely labeled BNST→CeA neurons we recorded from the $BNST_{OV}$ were identified as Type II neurons, and OT increased the frequency of sIPSCs in these Type II BNST→CeA neurons. Since all the BNST→CeA neurons we recorded from were identified as Type II, it is possible that Type II vs. Type III neurons target different subdivisions of the CeA as the BNST→CeA neurons were shown projecting to the CeL and the CeM (Gungor et al., 2015. It would still need to be determined which Type III projection neurons are affected by OT. Although neuropeptidergic phenotypes corresponding to Type I-III neurons remain elusive, Type III are putative corticotropin-releasing factor (CRF) neurons of the $BNST_{OV}$ (Dabrowska et al., 2013b), which were shown projecting to the LH, VTA, and the CeA, among many other brain regions (Dabrowska et al., 2016). Therefore, by reducing GABA-ergic transmission in Type III neurons, OT might increase probability of firing of these Type III/CRF projection neurons. However, as some CRF neurons in the $BNST_{DL}$ were also shown to serve as local interneurons

(Partridge et al., 2016), OT might have an excitatory influence on not just one (Type I) but possibly on two different types of $BNST_{DL}$ interneurons (Type I and Type III/CRF neurons). As a part of the future studies we will determine whether OT reduces GABA-ergic transmission in Type III interneurons vs. Type III projection neurons.

Notably, Type II neurons are the most abundant and heterogeneous neuronal population in rat $BNST_{DL}$ (Hazra et al., 2011; Yamauchi et al., 2018). The BNST is known to mediate stress-induced anxiety-like responses (Dabrowska et al., 2013b; Daniel and Rainnie, 2016; Davis et al., 2010; Sparta et al., 2013), contextual fear (Davis et al., 2010; Sullivan et al., 2004; Waddell et al., 2006), as well as fear responses to un-signaled, diffuse, or unpredictable threats (Duvarci et al., 2009; Goode et al., 2020, 2019), but might also inhibit cued fear responses to predictable threats (Meloni et al., 2006). Although the projection from the $BNST_{DL}$ to the CeA has been shown before (McDonald et al., 1999), a functional inhibitory projection was recently demonstrated (Gungor et al., 2015; Yamauchi et al., 2018), and was shown to facilitate anxiety-like behavior (Yamauchi et al., 2018). In apparent contrast to the BNST-mediated anxiety, our recent behavioral findings demonstrate that OTR transmission in the $BNST_{DL}$ reduces fear responses to un-signaled/diffuse threats and facilitates acquisition of cued fear (Janeček and Dabrowska, 2019; Martinon et al., 2019; Moaddab and Dabrowska, 2017). Based on the well-established role of the CeA in the acquisition of cued fear (Wilensky et al., 2006), our current electrophysiology results suggest that OTR activation in the $BNST_{DL}$ facilitates cued fear and reduces anxiety by inhibiting the Type II BNST→CeA output neurons. Therefore, our findings are of great significance for understanding the role of the BNST and its interactions with the CeA in the neurobiology of fear and anxiety and further highlight the unique potential of targeting oxytocin receptors for the treatment of anxiety disorders (Marvar et al., 2021).

5. Acknowledgements

We would like to thank Dr. Attilio Caravelli for his help with Matlab. We also thank Rachel Chudoba for proofreading the manuscript. This work was supported by grant from the National Institute of Mental Health R01MH113007 and R01MH113007-04S1 to JD and start-up funds from the Chicago Medical School, Rosalind Franklin University of Medicine and Science to JD.

6. Contributions

JD initiated the study. JD and WF designed the study. WF, FB, and VOP acquired data. WF, FB, VOP, and JD analyzed data. WF, FB, VOP and JD interpreted data. JD and WF wrote the manuscript. JD obtained funding.

7. Financial Disclosures

The authors declare no conflict of interest and have no financial interests to disclose. Dr. Joanna Dabrowska reports submission of a provisional patent application entitled: Method and System for Testing for Stress-related Mental Disorders, Susceptibility, Disease Progression, Disease Modulation and Treatment Efficacy (# 62/673447).

8. Figure legends

Figure 1. Oxytocin affects intrinsic membrane properties of Type I $BNST_{DL}$ neurons. A: Representative traces showing that oxytocin (OT, 0.2 μM) shortens the latency to the 1st spike at rheobase current (Rh) and depolarizes resting membrane potential (RMP, from -64 mV to -60 mV). This is associated with an increased input resistance (Rin), measured with a depolarizing current step below the Rh. OT also reduces Rh from 30 pA (pre) to 20 pA (OT) **B-F**: Line graphs with individual neurons responses (thin gray) and average responses for all neurons recorded (thick black) showing that OT significantly increases the RMP (**B**, P = 0.0002, F (1.593, 19.12) = 15.76, n = 14, mixed-effect analysis), increases Rin (**C**, P = 0.0085, n = 9, paired *t*-test), reduces the Rh (**D**, P = 0.0457, F (1.341, 16.09) = 4.226, n = 14, mixed-effect analysis), reduces the 1st spike threshold (**E**, P = 0.0164, F (1.472, 20.61) = 5.749, and reduces the 1st spike latency (**F**, P = 0.0185, F (1.971, 23.66) = 4.775, n = 14, mixed-effect analysis). Gray lines

represent individual neurons' responses to OT application. Thick black lines show average responses for all Type I neurons recorded, $^{**}P < 0.01$, $^{*}P < 0.05$ in comparison to pre or post-OT.

Figure 2. Oxytocin increases intrinsic excitability of Type I, but not Type II or Type III, $BNST_{DL}$ neurons. **A**: Representative traces showing voltage deflections in response to hyperpolarizing and depolarizing current injections characteristic of Type I neuron (left) and the increase in firing frequency of Type I neuron in the presence of OT respective to baseline (pre) (right). **B**: OT causes a leftward shift of input/output (I-O) relationship in Type I neurons. The steady state frequency (SSF) was determined as an average of an inverse of the inter-spike intervals (ISI) from all action potentials starting from the second action potential. In Type I neurons***,*** OT shows a significant increment effect on SSF at 40 pA ($P = 0.0024$, F (1.667, 15.01) = 10.11), at 50 pA ($P = 0.0271$, F (1.863, 16.76) = 4.628), and at 60 pA ($P = 0.0271$, F (1.688, 11.82) = 5.267, mixed-effects analysis). **C**: Application of OTR antagonist, OTA (0.4 μM), prevents the leftward shift of the I-O relationship induced by OT application (40 pA, $P = 0.3365$, 50 pA, $P = 0.4299$, 60 pA, $P = 0.6312$, n = 5, RM ANOVA). **D-E:** OT application does not modify the I-O relationship in Type II (**D**) or Type III $BNST_{DL}$ neurons (**E**). Each data point represents the mean ± SEM, $^{**}P < 0.01$, $^{*}P < 0.05$ in comparison to pre-OT, ## $P < 0.01$, # $P < 0.05$ in comparison to post-OT.

Figure 3. Oxytocin reduces fast and medium afterhyperpolarizations and modifies early and late spike frequency adaptation in Type I $BNST_{DL}$ neurons. **A**: Representative traces from Type I neuron showing a reduction of fast AHP (fAHP) and medium AHP (mAHP) after OT application respective to baseline (pre). The amplitudes of the fAHP and mAHP following the first action potential evoked at Rh were calculated as the difference from the action potential threshold to the membrane voltage measured after 2-5 msec and 50-100 msec, respectively. The lAHP was measured at 2000 msec after the end of the depolarizing pulse, following generation of five action potentials. **B**: Line graphs showing individual neurons' responses (gray)

and reduction of the fAHP during OT application (P = 0.0124, F (1.473, 17.68 = 6.493, mixed-effects analysis, n = 14). **C**: OTR antagonist, OTA (0.4 μM), prevents the OT-induced reduction of fAHP (P = 0.2220, n = 7, RM RM ANOVA). **D**: Line graph showing reduction of mAHP after OT application (P <0.0001, F (1.844, 22.13) = 23.25, mixed effect analysis, n = 14). **E***:* OT-induced reduction of mAHP is blocked by OTR antagonist, OTA (P = 0.3968, n = 7, RM ANOVA). Thick black lines show average responses for all Type I neurons recorded. **F**: OT modifies early and late spike frequency adaptation. The early and late spike frequency adaptation was investigated using a depolarizing pulse of 1 sec and measuring the instantaneous frequency for every action potential interval. The ISI number is the inter-stimulus interval between two consecutive action potentials. OT significantly increased the instantaneous frequency of ISI (P < 0.0001, F (1, 13) = 82.69, mixed effects model), **B-E**: Gray lines represent individual neurons' responses to OT application. Thick black lines show average responses for all Type I neurons recorded. **F**: Each data point represents the MEAN ± SEM, ****P < 0.0001, ***P < 0.001, **P < 0.01.

Figure 4. Oxytocin increases spontaneous firing rate of Type I neurons and reduces spontaneous firing rate of Type II $BNST_{DL}$ neurons in cell-attached recordings. **A**: Representative traces of Type I neuron showing an increase in spontaneous firing rate after OT application. **B**: Line graph showing that OT increased spontaneous firing rate in all spontaneously firing Type I neurons (P = 0.0242, paired t-test, n = 7). **C**: Representative traces of Type II neuron showing a reduction in spontaneous firing rate after OT application. **D**: Line graph showing that OT significantly reduced spontaneous firing rate in spontaneously firing Type II neurons in cell-attached mode (P = 0.0304, paired t-test, n = 7), gray lines represent individual neurons' responses, thick black line represents average response, *P < 0.05.

Figure 5. Oxytocin modulates inhibitory synaptic transmission in $BNST_{DL}$ neurons. A: Representative recordings from Type II neuron showing an increase in the frequency of spontaneous inhibitory postsynaptic currents (sIPSCs) after OT application respective to

baseline (pre). **B-C**: Line graphs (gray) showing that 12 out of 14 recorded Type II neurons showed an increase in sIPSCs frequency (**B**, P = 0.0022, F (1.058, 12.17) = 14.41, n = 14, mixed-effect analysis) but not amplitude (**C**, P = 0.5855, F (1.563, 17.19) = 0.4718, n = 14, mixed-effect analysis) after OT application. **D**: OT does not affect sIPSCs frequency in a presence of OTR antagonist, OTA (0.4 μM) (P = 0.1788, F (1.469, 8.814) = 2.135, n = 6, RM ANOVA). **E**: When spike-driven IPSCs were blocked with TTX (P = 0.0151, F (1.030, 6.179) = 10.98, n = 6, RM ANOVA), OT does not affect the sIPSCs frequency. **F-G**: OT does not affect frequency (**F**, P = 0.9362) but reduces amplitude of sIPSCs in Type III neurons (**G**, P = 0.0160, paired *t*-test. Gray lines represent individual neurons' responses to OT application. Thick black lines show average responses for all Type I neurons recorded, $^{**}P < 0.01$, $^{*}P < 0.05$ in comparison to pre- or post-OT.

Figure 6. Oxytocin reduces the amplitude of evoked IPSCs in Type III, but not Type II neurons. **A-B**: Representative traces of eIPSCs in response to electrical stimulation of the stria terminalis in Type II (**A**) and Type III (**B**) neurons. **C**: Line graph showing that OT does not change the mean amplitude of eIPSC in Type II neurons (P = 0.2459, paired *t*-test, n = 5). Thick black line shows averaged responses for all Type II neurons recorded. **D-G**: Line graphs showing responses of individual Type III neurons to OT application and the reduction of eIPSC amplitude (**D**, P = 0.0105, paired *t*-test, n = 6), without any significant change in the PPR (**E**, P = 0.5672). This effect of OT on eIPSCs amplitude was blocked by OTR antagonist, OTA (**F**, F (1.421, 7.105) = 0.1722, P = 0.7739, RM ANOVA, n = 6), but not by GABA-B receptor antagonist, CGP 55845 (**G**, F (1.258, 6.291) = 11.16, P = 0.0122, RM ANOVA, n = 6). Line graphs (gray lines) represent individual neurons' responses to treatment. Thick black lines show average responses for all neurons recorded.

Figure 7. Oxytocin inhibits Type II BNST→CeA output neurons. **A-B**: Microphotographs showing a representative injection site of green retrobeads in the central amygdala (CeA, here visualized with enkephalin immunofluorescence in red, **A**, scale bar 100 μm) and neurons

expressing green fluorescent microbeads in the $BNST_{DL}$ (**B**, bar 100 μm). BNST neurons projecting to the CeA (BNST→CeA neurons) are found in the dorsolateral BNST, primarily the oval nucleus ($BNST_{OV}$), and to a lesser extent in the anteromedial BNST ($BNST_{AM}$) (BLA – basolateral nucleus of the amygdala, IC – Internal capsule, LV – Lateral ventricle). **C**: High magnification (60x) microphotographs obtained from a confocal microscope showing green fluorescent beads present in membranes and processes of the BNST→CeA neurons (scale bar 10 μm). **D-E**: Electrophysiological characterization of the BNST→CeA neurons using visually guided patching (**D**, 40x, scale bar 10 μm). Representative recording of the BNST→CeA fluorescent neuron showing the electrophysiological properties of a Type II neuron such as the presence of a sag during the hyperpolarized current pulses and the spike rebound at the end of the 450 msec current pulse injection (**E**). **F**: OT increases the frequency of sIPSCs (F (1.004, 4.016) = 10.99, P = 0.0293, RM ANOVA, n = 5) in the fluorescent Type II BNST→CeA neurons. Gray lines represent individual neurons' responses to treatment. Thick black lines show average responses for all Type II neurons recorded. **G**: Diagram showing that OT regulates the intrinsic inhibitory network of the $BNST_{DL}$. By directly increasing spontaneous firing of Type I regular spiking interneurons, OT reduces firing of Type II $BNST_{DL}$ neurons, which send projections to the central amygdala (BNST→CeA neurons*)*. OT also reduces the evoked GABA-ergic inhibition in Type III $BNST_{DL}$ neurons, via a direct postsynaptic mechanism.

9. References

al-Shamma, H.A., De Vries, G.J., 1996. Neurogenesis of the sexually dimorphic vasopressin cells of the bed nucleus of the stria terminalis and amygdala of rats. J. Neurobiol. 29, 91–98. https://doi.org/10.1002/(SICI)1097-4695(199601)29:1<91::AID-NEU7>3.0.CO;2-2

Alger, B.E., Nicoll, R.A., 1980. Epileptiform burst afterhyperolarization: calcium-dependent potassium potential in hippocampal CA1 pyramidal cells. Science 210, 1122–1124. https://doi.org/10.1126/science.7444438

Alheid, G.F., 2003. Extended amygdala and basal forebrain. Ann. N. Y. Acad. Sci. 985, 185–205.

Beyeler, A., Dabrowska, J., 2020. Neuronal diversity of the amygdala and the bed nucleus of the stria terminalis. Handb Behav Neurosci 26, 63–100. https://doi.org/10.1016/b978-0-12-815134-1.00003-9

Bosch, O.J., Young, L.J., 2018. Oxytocin and Social Relationships: From Attachment to Bond Disruption. Curr Top Behav Neurosci 35, 97–117. https://doi.org/10.1007/7854_2017_10

Brussaard, A.B., Kits, K.S., de Vlieger, T.A., 1996. Postsynaptic mechanism of depression of GABAergic synapses by oxytocin in the supraoptic nucleus of immature rat. J Physiol 497 (Pt 2), 495–507. https://doi.org/10.1113/jphysiol.1996.sp021783

Caldeyro-Barcia, R., Poseiro, J.J., 1959. Oxytocin and contractility of the pregnant human uterus. Ann. N. Y. Acad. Sci. 75, 813–830.

Crane, J.W., Holmes, N.M., Fam, J., Westbrook, R.F., Delaney, A.J., 2020. Oxytocin increases inhibitory synaptic transmission and blocks development of long-term potentiation in the lateral amygdala. J. Neurophysiol. 123, 587–599. https://doi.org/10.1152/jn.00571.2019

Cullinan, W.E., Herman, J.P., Watson, S.J., 1993. Ventral subicular interaction with the hypothalamic paraventricular nucleus: evidence for a relay in the bed nucleus of the stria terminalis. J. Comp. Neurol. 332, 1–20. https://doi.org/10.1002/cne.903320102

Dabrowska, J., Hazra, R., Ahern, T.H., Guo, J.-D., McDonald, A.J., Mascagni, F., Muller, J.F., Young, L.J., Rainnie, D.G., 2011. Neuroanatomical evidence for reciprocal regulation of the corticotrophin-releasing factor and oxytocin systems in the hypothalamus and the bed nucleus of the stria terminalis of the rat: Implications for balancing stress and affect. Psychoneuroendocrinology 36, 1312–1326. https://doi.org/10.1016/j.psyneuen.2011.03.003

Dabrowska, J., Hazra, R., Guo, J.-D., Dewitt, S., Rainnie, D.G., 2013a. Central CRF neurons are not created equal: phenotypic differences in CRF-containing neurons of the rat paraventricular hypothalamus and the bed nucleus of the stria terminalis. Front Neurosci 7, 156. https://doi.org/10.3389/fnins.2013.00156

Dabrowska, J., Hazra, R., Guo, J.-D., Li, C., Dewitt, S., Xu, J., Lombroso, P.J., Rainnie, D.G., 2013b. Striatal-enriched protein tyrosine phosphatase-STEPs toward understanding chronic stress-induced activation of corticotrophin releasing factor neurons in the rat bed nucleus of the stria terminalis. Biol. Psychiatry 74, 817–826. https://doi.org/10.1016/j.biopsych.2013.07.032

Dabrowska, J., Martinon, D., Moaddab, M., Rainnie, D.G., 2016. Targeting Corticotropin-Releasing Factor Projections from the Oval Nucleus of the Bed Nucleus of the Stria Terminalis Using Cell-Type Specific Neuronal Tracing Studies in Mouse and Rat Brain. J. Neuroendocrinol. 28. https://doi.org/10.1111/jne.12442

Daniel, S.E., Guo, J., Rainnie, D.G., 2017. A comparative analysis of the physiological properties of neurons in the anterolateral bed nucleus of the stria terminalis in the Mus musculus, Rattus norvegicus, and Macaca mulatta. J. Comp. Neurol. 525, 2235–2248. https://doi.org/10.1002/cne.24202

Daniel, S.E., Rainnie, D.G., 2016. Stress Modulation of Opposing Circuits in the Bed Nucleus of the Stria Terminalis. Neuropsychopharmacology 41, 103–125. https://doi.org/10.1038/npp.2015.178

Davis, M., Walker, D.L., Miles, L., Grillon, C., 2010. Phasic vs sustained fear in rats and humans: role of the extended amygdala in fear vs anxiety. Neuropsychopharmacology 35, 105–135. https://doi.org/10.1038/npp.2009.109

Dumais, K.M., Bredewold, R., Mayer, T.E., Veenema, A.H., 2013. Sex differences in oxytocin receptor binding in forebrain regions: correlations with social interest in brain region- and sex- specific ways. Horm Behav 64, 693–701. https://doi.org/10.1016/j.yhbeh.2013.08.012

Duvarci, S., Bauer, E.P., Paré, D., 2009. The bed nucleus of the stria terminalis mediates inter-individual variations in anxiety and fear. J. Neurosci. 29, 10357–10361. https://doi.org/10.1523/JNEUROSCI.2119-09.2009

Francesconi, W., Berton, F., Repunte-Canonigo, V., Hagihara, K., Thurbon, D., Lekic, D., Specio, S.E., Greenwell, T.N., Chen, S.A., Rice, K.C., Richardson, H.N., O'Dell, L.E., Zorrilla, E.P., Morales, M., Koob, G.F., Sanna, P.P., 2009. Protracted withdrawal from alcohol and drugs of abuse impairs long-term potentiation of intrinsic excitability in the juxtacapsular bed nucleus of the stria terminalis. J. Neurosci. 29, 5389–5401. https://doi.org/10.1523/JNEUROSCI.5129-08.2009

Goode, T.D., Acca, G.M., Maren, S., 2020. Threat imminence dictates the role of the bed nucleus of the stria terminalis in contextual fear. Neurobiol Learn Mem 167, 107116. https://doi.org/10.1016/j.nlm.2019.107116

Goode, T.D., Ressler, R.L., Acca, G.M., Miles, O.W., Maren, S., 2019. Bed nucleus of the stria terminalis regulates fear to unpredictable threat signals. Elife 8. https://doi.org/10.7554/eLife.46525

Gozzi, A., Jain, A., Giovannelli, A., Giovanelli, A., Bertollini, C., Crestan, V., Schwarz, A.J., Tsetsenis, T., Ragozzino, D., Gross, C.T., Bifone, A., 2010. A neural switch for active and passive fear. Neuron 67, 656–666. https://doi.org/10.1016/j.neuron.2010.07.008

Grundwald, N.J., Benítez, D.P., Brunton, P.J., 2016. Sex-Dependent Effects of Prenatal Stress on Social Memory in Rats: A Role for Differential Expression of Central Vasopressin-1a Receptors. J. Neuroendocrinol. 28. https://doi.org/10.1111/jne.12343

Gu, N., Hu, H., Vervaeke, K., Storm, J.F., 2008. SK (KCa2) channels do not control somatic excitability in CA1 pyramidal neurons but can be activated by dendritic excitatory synapses and regulate their impact. J. Neurophysiol. 100, 2589–2604. https://doi.org/10.1152/jn.90433.2008

Gu, N., Vervaeke, K., Hu, H., Storm, J.F., 2005a. Kv7/KCNQ/M and HCN/h, but not KCa2/SK channels, contribute to the somatic medium after-hyperpolarization and excitability control in CA1 hippocampal pyramidal cells. J. Physiol. (Lond.) 566, 689–715. https://doi.org/10.1113/jphysiol.2005.086835

Gu, N., Vervaeke, K., Hu, H., Storm, J.F., 2005b. Kv7/KCNQ/M and HCN/h, but not KCa2/SK channels, contribute to the somatic medium after-hyperpolarization and excitability control in CA1 hippocampal pyramidal cells. J. Physiol. (Lond.) 566, 689–715. https://doi.org/10.1113/jphysiol.2005.086835

Gu, N., Vervaeke, K., Storm, J.F., 2007. BK potassium channels facilitate high-frequency firing and cause early spike frequency adaptation in rat CA1 hippocampal pyramidal cells. J. Physiol. (Lond.) 580, 859–882. https://doi.org/10.1113/jphysiol.2006.126367

Gungor, N.Z., Paré, D., 2016. Functional Heterogeneity in the Bed Nucleus of the Stria Terminalis. J. Neurosci. 36, 8038–8049. https://doi.org/10.1523/JNEUROSCI.0856-16.2016

Gungor, N.Z., Yamamoto, R., Paré, D., 2015. Optogenetic study of the projections from the bed nucleus of the stria terminalis to the central amygdala. J. Neurophysiol. 114, 2903–2911. https://doi.org/10.1152/jn.00677.2015

Hammack, S.E., Mania, I., Rainnie, D.G., 2007. Differential expression of intrinsic membrane currents in defined cell types of the anterolateral bed nucleus of the stria terminalis. J. Neurophysiol. 98, 638–656. https://doi.org/10.1152/jn.00382.2007

Han, J.S., Maeda, Y., Knepper, M.A., 1993. Dual actions of vasopressin and oxytocin in regulation of water permeability in terminal collecting duct. Am. J. Physiol. 265, F26-34. https://doi.org/10.1152/ajprenal.1993.265.1.F26

Harden, S.W., Frazier, C.J., 2016. Oxytocin depolarizes fast-spiking hilar interneurons and induces GABA release onto mossy cells of the rat dentate gyrus. Hippocampus 26, 1124–1139. https://doi.org/10.1002/hipo.22595

Huber, D., Veinante, P., Stoop, R., 2005. Vasopressin and oxytocin excite distinct neuronal populations in the central amygdala. Science 308, 245–248. https://doi.org/10.1126/science.1105636

Hung, L.W., Neuner, S., Polepalli, J.S., Beier, K.T., Wright, M., Walsh, J.J., Lewis, E.M., Luo, L., Deisseroth, K., Dölen, G., Malenka, R.C., 2017. Gating of social reward by oxytocin in

the ventral tegmental area. Science 357, 1406–1411. https://doi.org/10.1126/science.aan4994

Ingram, C.D., Cutler, K.L., Wakerley, J.B., 1990. Oxytocin excites neurones in the bed nucleus of the stria terminalis of the lactating rat in vitro. Brain Res. 527, 167–170.

Ingram, C.D., Moos, F., 1992. Oxytocin-containing pathway to the bed nuclei of the stria terminalis of the lactating rat brain: immunocytochemical and in vitro electrophysiological evidence. Neuroscience 47, 439–452.

Janeček, M., Dabrowska, J., 2019. Oxytocin facilitates adaptive fear and attenuates anxiety responses in animal models and human studies-potential interaction with the corticotropin-releasing factor (CRF) system in the bed nucleus of the stria terminalis (BNST). Cell Tissue Res. 375, 143–172. https://doi.org/10.1007/s00441-018-2889-8

Knobloch, H.S., Charlet, A., Hoffmann, L.C., Eliava, M., Khrulev, S., Cetin, A.H., Osten, P., Schwarz, M.K., Seeburg, P.H., Stoop, R., Grinevich, V., 2012. Evoked axonal oxytocin release in the central amygdala attenuates fear response. Neuron 73, 553–566. https://doi.org/10.1016/j.neuron.2011.11.030

Kremarik, P., Freund-Mercier, M.J., Stoeckel, M.E., 1991. Autoradiographic detection of oxytocin- and vasopressin-binding sites in various subnuclei of the bed nucleus of the stria terminalis in the rat. Effects of functional and experimental sexual steroid variations. J. Neuroendocrinol. 3, 689–698. https://doi.org/10.1111/j.1365-2826.1991.tb00335.x

Lopez de Armentia, M., Sah, P., 2004. Firing properties and connectivity of neurons in the rat lateral central nucleus of the amygdala. J. Neurophysiol. 92, 1285–1294. https://doi.org/10.1152/jn.00211.2004

Maejima, S., Ohishi, N., Yamaguchi, S., Tsukahara, S., 2015. A neural connection between the central part of the medial preoptic nucleus and the bed nucleus of the stria terminalis to regulate sexual behavior in male rats. Neurosci. Lett. 606, 66–71. https://doi.org/10.1016/j.neulet.2015.08.047

Maniezzi, C., Talpo, F., Spaiardi, P., Toselli, M., Biella, G., 2019. Oxytocin Increases Phasic and Tonic GABAergic Transmission in CA1 Region of Mouse Hippocampus. Front Cell Neurosci 13, 178. https://doi.org/10.3389/fncel.2019.00178

Manning, M., Misicka, A., Olma, A., Bankowski, K., Stoev, S., Chini, B., Durroux, T., Mouillac, B., Corbani, M., Guillon, G., 2012. Oxytocin and vasopressin agonists and antagonists as research tools and potential therapeutics. J. Neuroendocrinol. 24, 609–628. https://doi.org/10.1111/j.1365-2826.2012.02303.x

Marlin, B.J., Mitre, M., D'amour, J.A., Chao, M.V., Froemke, R.C., 2015. Oxytocin enables maternal behaviour by balancing cortical inhibition. Nature 520, 499–504. https://doi.org/10.1038/nature14402

Martina, M., Kilić, G., Cherubini, E., 1994. The effect of intracellular Ca2+ on GABA-activated currents in cerebellar granule cells in culture. J. Membr. Biol. 142, 209–216. https://doi.org/10.1007/BF00234942

Martinon, D., Lis, P., Roman, A.N., Tornesi, P., Applebey, S.V., Buechner, G., Olivera, V., Dabrowska, J., 2019. Oxytocin receptors in the dorsolateral bed nucleus of the stria terminalis (BNST) bias fear learning toward temporally predictable cued fear. Transl Psychiatry 9, 140. https://doi.org/10.1038/s41398-019-0474-x

Marvar, P.J., Andero, R., Hurlemann, R., Lago, T.R., Zelikowsky, M., Dabrowska, J., 2021. Limbic Neuropeptidergic Modulators of Emotion and Their Therapeutic Potential for Anxiety and Post-Traumatic Stress Disorder. J Neurosci 41, 901–910. https://doi.org/10.1523/JNEUROSCI.1647-20.2020

McDonald, A.J., Shammah-Lagnado, S.J., Shi, C., Davis, M., 1999. Cortical afferents to the extended amygdala. Ann. N. Y. Acad. Sci. 877, 309–338.

Meloni, E.G., Jackson, A., Gerety, L.P., Cohen, B.M., Carlezon, W.A., 2006. Role of the bed nucleus of the stria terminalis (BST) in the expression of conditioned fear. Ann. N. Y. Acad. Sci. 1071, 538–541. https://doi.org/10.1196/annals.1364.059

Moaddab, M., Dabrowska, J., 2017. Oxytocin receptor neurotransmission in the dorsolateral bed nucleus of the stria terminalis facilitates the acquisition of cued fear in the fear-potentiated startle paradigm in rats. Neuropharmacology 121, 130–139. https://doi.org/10.1016/j.neuropharm.2017.04.039

Nakajima, M., Görlich, A., Heintz, N., 2014. Oxytocin modulates female sociosexual behavior through a specific class of prefrontal cortical interneurons. Cell 159, 295–305. https://doi.org/10.1016/j.cell.2014.09.020

Neumann, I.D., Slattery, D.A., 2016. Oxytocin in General Anxiety and Social Fear: A Translational Approach. Biol. Psychiatry 79, 213–221. https://doi.org/10.1016/j.biopsych.2015.06.004

Nickerson, K., Bonsness, R.W., Douglas, R.G., Condliffe, P., Du Vigneaud, V., 1954. Oxytocin and milk ejection. Am. J. Obstet. Gynecol. 67, 1028–1034.

Okamura, H., Abitbol, M., Julien, J.F., Dumas, S., Bérod, A., Geffard, M., Kitahama, K., Bobillier, P., Mallet, J., Wiklund, L., 1990. Neurons containing messenger RNA encoding glutamate decarboxylase in rat hypothalamus demonstrated by in situ hybridization, with special emphasis on cell groups in medial preoptic area, anterior hypothalamic area and dorsomedial hypothalamic nucleus. Neuroscience 39, 675–699. https://doi.org/10.1016/0306-4522(90)90252-y

Olivera-Pasilio, V., Dabrowska, J., 2020. Oxytocin Promotes Accurate Fear Discrimination and Adaptive Defensive Behaviors. Front. Neurosci. 14, 583878. https://doi.org/10.3389/fnins.2020.583878

Owen, S.F., Tuncdemir, S.N., Bader, P.L., Tirko, N.N., Fishell, G., Tsien, R.W., 2013. Oxytocin enhances hippocampal spike transmission by modulating fast-spiking interneurons. Nature 500, 458–462. https://doi.org/10.1038/nature12330

Partridge, J.G., Forcelli, P.A., Luo, R., Cashdan, J.M., Schulkin, J., Valentino, R.J., Vicini, S., 2016. Stress increases GABAergic neurotransmission in CRF neurons of the central amygdala and bed nucleus stria terminalis. Neuropharmacology 107, 239–250. https://doi.org/10.1016/j.neuropharm.2016.03.029

Pedarzani, P., Storm, J.F., 1993. PKA mediates the effects of monoamine transmitters on the K+ current underlying the slow spike frequency adaptation in hippocampal neurons. Neuron 11, 1023–1035. https://doi.org/10.1016/0896-6273(93)90216-e

Pedersen, C.A., Caldwell, J.D., Peterson, G., Walker, C.H., Mason, G.A., 1992. Oxytocin activation of maternal behavior in the rat. Ann. N. Y. Acad. Sci. 652, 58–69.

Perkins, K.L., 2006. Cell-attached voltage-clamp and current-clamp recording and stimulation techniques in brain slices. J. Neurosci. Methods 154, 1–18. https://doi.org/10.1016/j.jneumeth.2006.02.010

Rodríguez-Sierra, O.E., Turesson, H.K., Pare, D., 2013. Contrasting distribution of physiological cell types in different regions of the bed nucleus of the stria terminalis. J. Neurophysiol. 110, 2037–2049. https://doi.org/10.1152/jn.00408.2013

Sharma, K., LeBlanc, R., Haque, M., Nishimori, K., Reid, M.M., Teruyama, R., 2019. Sexually dimorphic oxytocin receptor-expressing neurons in the preoptic area of the mouse brain. PLoS ONE 14, e0219784. https://doi.org/10.1371/journal.pone.0219784

Simerly, R.B., Swanson, L.W., 1988. Projections of the medial preoptic nucleus: a Phaseolus vulgaris leucoagglutinin anterograde tract-tracing study in the rat. J. Comp. Neurol. 270, 209–242. https://doi.org/10.1002/cne.902700205

Sparta, D.R., Jennings, J.H., Ung, R.L., Stuber, G.D., 2013. Optogenetic strategies to investigate neural circuitry engaged by stress. Behav. Brain Res. 255, 19–25. https://doi.org/10.1016/j.bbr.2013.05.007

Sullivan, G.M., Apergis, J., Bush, D.E.A., Johnson, L.R., Hou, M., Ledoux, J.E., 2004. Lesions in the bed nucleus of the stria terminalis disrupt corticosterone and freezing responses elicited by a contextual but not by a specific cue-conditioned fear stimulus. Neuroscience 128, 7–14. https://doi.org/10.1016/j.neuroscience.2004.06.015

Sun, N., Cassell, M.D., 1993. Intrinsic GABAergic neurons in the rat central extended amygdala. J. Comp. Neurol. 330, 381–404. https://doi.org/10.1002/cne.903300308

Tabbaa, M., Paedae, B., Liu, Y., Wang, Z., 2016. Neuropeptide Regulation of Social Attachment: The Prairie Vole Model. Compr Physiol 7, 81–104. https://doi.org/10.1002/cphy.c150055

Terburg, D., Scheggia, D., Triana Del Rio, R., Klumpers, F., Ciobanu, A.C., Morgan, B., Montoya, E.R., Bos, P.A., Giobellina, G., van den Burg, E.H., de Gelder, B., Stein, D.J., Stoop, R., van Honk, J., 2018. The Basolateral Amygdala Is Essential for Rapid Escape: A Human and Rodent Study. Cell 175, 723-735.e16. https://doi.org/10.1016/j.cell.2018.09.028

Tirko, N.N., Eyring, K.W., Carcea, I., Mitre, M., Chao, M.V., Froemke, R.C., Tsien, R.W., 2018. Oxytocin Transforms Firing Mode of CA2 Hippocampal Neurons. Neuron 100, 593-608.e3. https://doi.org/10.1016/j.neuron.2018.09.008

Tribollet, E., Dubois-Dauphin, M., Dreifuss, J.J., Barberis, C., Jard, S., 1992. Oxytocin receptors in the central nervous system. Distribution, development, and species differences. Ann. N. Y. Acad. Sci. 652, 29–38.

Tunstall, B.J., Kirson, D., Zallar, L.J., McConnell, S.A., Vendruscolo, J.C.M., Ho, C.P., Oleata, C.S., Khom, S., Manning, M., Lee, M.R., Leggio, L., Koob, G.F., Roberto, M., Vendruscolo, L.F., 2019. Oxytocin blocks enhanced motivation for alcohol in alcohol dependence and blocks alcohol effects on GABAergic transmission in the central amygdala. PLoS Biol 17, e2006421. https://doi.org/10.1371/journal.pbio.2006421

Veinante, P., Freund-Mercier, M.J., 1997. Distribution of oxytocin- and vasopressin-binding sites in the rat extended amygdala: a histoautoradiographic study. J. Comp. Neurol. 383, 305–325.

Verbalis, J.G., Blackburn, R.E., Olson, B.R., Stricker, E.M., 1993. Central oxytocin inhibition of food and salt ingestion: a mechanism for intake regulation of solute homeostasis. Regul. Pept. 45, 149–154.

Viviani, D., Charlet, A., van den Burg, E., Robinet, C., Hurni, N., Abatis, M., Magara, F., Stoop, R., 2011. Oxytocin selectively gates fear responses through distinct outputs from the central amygdala. Science 333, 104–107. https://doi.org/10.1126/science.1201043

Waddell, J., Morris, R.W., Bouton, M.E., 2006. Effects of bed nucleus of the stria terminalis lesions on conditioned anxiety: aversive conditioning with long-duration conditional stimuli and reinstatement of extinguished fear. Behav. Neurosci. 120, 324–336. https://doi.org/10.1037/0735-7044.120.2.324

Wilensky, A.E., Schafe, G.E., Kristensen, M.P., LeDoux, J.E., 2006. Rethinking the fear circuit: the central nucleus of the amygdala is required for the acquisition, consolidation, and expression of Pavlovian fear conditioning. J Neurosci 26, 12387–12396. https://doi.org/10.1523/JNEUROSCI.4316-06.2006

Wilson, B.C., Terenzi, M.G., Ingram, C.D., 2005. Differential excitatory responses to oxytocin in sub-divisions of the bed nuclei of the stria terminalis. Neuropeptides 39, 403–407. https://doi.org/10.1016/j.npep.2005.04.001

Xiao, L., Priest, M.F., Nasenbeny, J., Lu, T., Kozorovitskiy, Y., 2017. Biased Oxytocinergic Modulation of Midbrain Dopamine Systems. Neuron 95, 368-384.e5. https://doi.org/10.1016/j.neuron.2017.06.003

Xu, X., Ikrar, T., Sun, Y., Santos, R., Holmes, T.C., Francesconi, W., Berton, F., 2016. High-resolution and cell-type-specific photostimulation mapping shows weak excitatory vs. strong inhibitory inputs in the bed nucleus of the stria terminalis. J. Neurophysiol. 115, 3204–3216. https://doi.org/10.1152/jn.01148.2015

Yamauchi, N., Takahashi, D., Sugimura, Y.K., Kato, F., Amano, T., Minami, M., 2018. Activation of the neural pathway from the dorsolateral bed nucleus of the stria terminalis to the central amygdala induces anxiety-like behaviors. Eur. J. Neurosci. 48, 3052–3061. https://doi.org/10.1111/ejn.14165

Zaninetti, M., Raggenbass, M., 2000. Oxytocin receptor agonists enhance inhibitory synaptic transmission in the rat hippocampus by activating interneurons in stratum pyramidale. Eur. J. Neurosci. 12, 3975–3984. https://doi.org/10.1046/j.1460-9568.2000.00290.x